Genetic analysis of vitamin D related genes in Canadian multiple sclerosis patients

Article abstract—The objective of this study was to investigate genes involved in the metabolism and function of vitamin D as candidate genes for genetic susceptibility to MS. Restriction fragment length polymorphisms and highly polymorphic microsatellite markers within or very close to the $1,25(OH)_2D_3$ receptor (VDR) [12q14], the vitamin D binding protein (DBP) [4q12], and the $25(OH)D_3$ 1α-hydroxylase [12q13] loci were analyzed for linkage or association with MS. We found no evidence for linkage or association of these candidate genes with MS in the Canadian population. **Key words:** Vitamin D—MS.

NEUROLOGY 2000;54:729–732

J.L. Steckley, MSc; D.A. Dyment, MSc; A.D. Sadovnick, PhD; N. Risch, PhD; C. Hayes, PhD; G.C. Ebers, MD, FRCP(C); and the Canadian Collaborative Study Group*

Multiple sclerosis is a demyelinating disease of the CNS with a suspected autoimmune mechanism. MS has a marked geographical distribution with low prevalence in equatorial regions and an increasing prevalence with latitude.[1] It has been suggested that increased exposure to solar radiation may have a protective effect on MS.[2] At low latitude, solar radiation may provide the essential amount of vitamin D through biosynthesis in the skin and protect genetically susceptible individuals from developing MS. A high prevalence of vitamin D deficiency has been demonstrated in MS patients, supporting this theory.[3] In addition, in vivo experiments with experimental autoimmune encephalitis mice show that exogenous vitamin D hormone, $1,25(OH)_2D_3$, dramatically inhibits disease induction and progression.[4] A recent hypothesis has unified these ideas, suggesting that $1,25(OH)_2D_3$ is a selective immune system regulator essential for protecting against MS.[5]

Familial aggregation of MS is largely genetically determined,[6] and various genes have been analyzed to locate MS susceptibility loci. Candidate gene studies have focused on genes of immune cell function (T cell receptor, immunoglobulin, complement, and TNF-α) and potential CNS antigens (myelin basic protein). We have focused on genes involved in the metabolism and function of vitamin D—the vitamin D binding protein (DBP), the vitamin D receptor (VDR), and the $25(OH)D_3$ 1α-hydroxylase. Vitamin D binding protein and 1α-hydroxylase are essential for the transport and production of $1,25(OH)_2D_3$[5] (figure), while the VDR is necessary to mediate the actions of $1,25(OH)_2D_3$. We have analyzed the VDR, DBP, and 1α-hydroxylase loci with the transmission disequilibrium test (TDT) and with linkage methods.

Materials and methods. The Canadian Collaborative Project on Genetic Susceptibility to Multiple Sclerosis (CCPGSMS) has screened over 16,000 MS patients in 15 population-based clinics across Canada. Family history information was obtained through telephone interviews. Patients with other affected family members were identified and medical records were obtained in order to confirm the diagnoses. Whenever possible, the affected relative was diagnosed by a neurologist with expertise in the differential diagnosis of MS at one of the 15 regional centers. Blood samples were collected with informed consent from affected pairs, unaffected siblings, and available parents. Genomic DNA was extracted from peripheral blood samples using standard conditions. In all, 236 sibling pairs from 187 families were analyzed in this study. For additional information, please see our Web site (www.neurology.org). For the microsatellite markers, the four most common alleles were analyzed by the TDT. The p value for the multiple comparisons was corrected according to the Bonferroni procedure ($p = 0.0125$). All restriction fragment length polymorphisms (RFLPs) were also analyzed by the TDT ($p = 0.05$). After transmission disequilibrium testing, two-point and multipoint analysis of the

Additional material related to this article can be found on the *Neurology* Web site. Go to www.neurology.org and then scroll down the Table of Contents for the February 8 issue to find the title link for this article.

*See the Appendix on page 731 for a listing of members of the Canadian Collaborative Study Group.

From the Wellcome Trust Centre for Human Genetics (Drs. Steckley and Dyment) and the Department of Clinical Neurology (Dr. Ebers), University of Oxford, Oxford, England; the Department of Medical Genetics (Dr. Sadovnick), University of British Columbia, Vancouver, British Columbia, Canada; the Department of Genetics (Dr. Risch), Stanford University, Palo Alto, CA; and the Department of Biochemistry (Dr. Hayes), University of Wisconsin-Madison.

Supported by the Multiple Sclerosis Society of Canada Scientific Research Foundation.

Received April 19, 1999. Accepted in final form August 19, 1999.

Address correspondence and reprint requests to Professor George C. Ebers, University of Oxford, Department of Clinical Neurology, Radcliffe Infirmary, Woodstock Road, Oxford, 0X2 6HE, England.

See also pages 542 and 552

Copyright © 2000 by the American Academy of Neurology

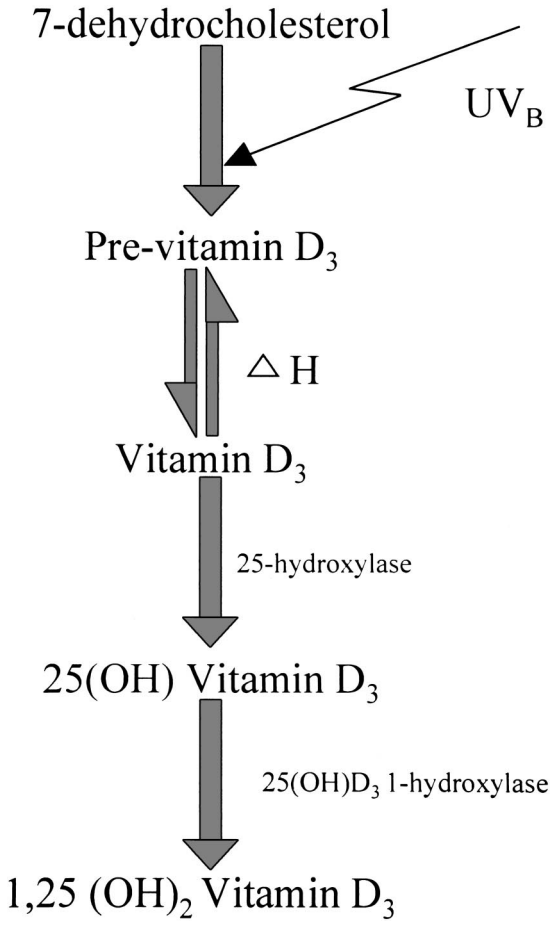

Figure. The biosynthesis of 1,25(OH)$_2$D$_3$: 7-dehydrocholesterol absorbs UV light that ruptures a bond leading to previtamin D$_3$ formation in the skin. Previtamin D$_3$ isomerizes to form vitamin D3, which is transported bound to DBP. Vitamin D$_3$ is transported to the liver where it is 25-hydroxylated by a constituitively expressed enzyme. 25(OH)D$_3$ is transported to the kidney, where a 1α-hydoxylase converts it to the hormonally active form, 1,25(OH)$_2$D$_3$.

data was carried out. Linkage disequilibrium testing and linkage analysis was completed using the sib_tdt and sib_ibd programs of the ASPEX statistical package.

Results. Four microsatellite markers and four RFLPs were genotyped in 187 families with MS. A TDT resulted in varying numbers of informative families from marker to marker, because the test relies on the transmissions of a given allele from heterozygous parents to affected offspring. Markers with differing heterozygosities will result in differing numbers of heterozygous parents. For maximum likelihood identity-by-descent analysis, 184 families were informative.

At the VDR locus, TDT analysis of the *Apa*I and *Taq*I polymorphisms did not show preferential transmission of any allele to affected offspring (table 1). Two-point linkage analysis yielded mlod values of 0.54 and 0.10, respectively (table 2). For D12S85, no deviation in the transmission of alleles was seen (table 1). Two-point linkage analysis yielded an mlod of 0.01 (table 2). Multipoint identity-by-descent analysis of D12S85 as well as the *Taq*I and *Apa*I polymorphisms yielded negative lod scores, excluding the VDR gene from contributing a λ value (recurrence risk of sib/population prevalence) greater than 1.75.

Within the DBP gene, TDT analysis of the *Hae*III and *Sty*I genotypes showed no preferential transmission of any allele to affected offspring (table 1). Two-point linkage analysis of the *Hae*III and *Sty*I polymorphisms was negative, as shown by the mlod scores of 0.00 in table 2. Multipoint identity-by-descent analysis excluded the DBP gene from contributing a λ value greater than 1.75.

At the 1α-hydroxylase locus, three nearby microsatellite markers (D12S90, D12S355, and D12S83) were analyzed. A TDT analysis of the four most common alleles for each marker showed a slight difference in transmission for allele 10 ($p = 0.008637$) of marker D12S355 (table 1). All other alleles for D12S355 and all alleles of markers D12S85, D12S90, and D12S83 showed no deviation in transmission. Two-point linkage analysis yielded mlod scores of 0.00 for each microsatellite marker (table 2). Multipoint identity-by-descent analysis excluded the 1α-hydroxylase gene from contributing a λ value greater than 1.50.

Discussion. We evaluated three genes encoding proteins involved in vitamin D metabolism and function; the VDR gene (12q14), the DBP gene (4q12), and the 1α-hydroxylase gene (12q13). We evaluated the distribution of *Apa*I and *Taq*I RFLPs within a 740 bp segment of the VDR gene. No significant deviation from expected transmission of alleles to affected offspring was observed. Two-point linkage analysis failed to detect linkage and multipoint analysis excluded the VDR gene as a susceptibility gene contributing a λ value greater than 1.75. A microsatellite marker, D12S85, within 2 cm of the VDR locus also did not show linkage disequilibrium. Multipoint and two-point linkage analysis of D12S85 also failed to detect linkage. Our observations exclude the VDR as a significant MS susceptibility locus in Canadians and suggest that polymorphisms in the VDR do not contribute to MS susceptibility in this population.

The association of the DBP protein with MS has previously been analyzed, as the Gc-1f allele of DBP was associated with MS in a comparison of 63 Icelandic MS patients with 40 of their relatives.[7] In our study, TDT analysis of the *Hae*III and *Sty*I RFLPs showed no deviation in transmission of alleles to affected offspring. Similarly, two-point and multipoint linkage analysis also showed no linkage of the DBP gene with MS. The lack of association in the Canadian population conflicts with the Icelandic study. Given our negative results in a larger, more conclusive sample size of 236 sib pairs, the gene for DBP is not likely a major MS susceptibility locus.

For the 1α-hydroxylase locus, we genotyped three microsatellite markers. D12S355 and D12S83 are all located within 1 cM of the 1α-hydroxylase locus, while D12S90 is 3 cm away.[8] Allele 10 of microsatellite marker D12S355 was the only allele transmitted to offspring from heterozygous parents in a ratio different than the expected ($p = 0.00864$). However,

Table 1 *Transmission disequilibrium testing of the restriction fragment length polymorphisms and the four most common alleles for the microsatellite markers at the DBP, VDR, and 1α-hydroxylase loci*

Locus	Marker	H	Allele (size)	N	% Freq	TR	NT	Chi^2	*p* Value
VDR	*Taq*I	0.488		187	37.7	98	83	1.2	0.273
	*Apa*I	0.447		250	49.2	73	95	2.9	0.089
	D12S85	0.632	1 (105 bp)	282	54.9	99	118	1.7	0.192
			7 (117 bp)	82	16.0	62	63	0.0	1.000
			8 (119 bp)	49	9.5	43	26	4.2	0.040
			10 (133 bp)	47	9.1	39	38	0.0	1.000
DBP	*Hae*III	0.488		266	51.6	86	100	1.1	0.273
	*Sty*I	0.411		166	31.6	86	80	0.2	0.655
1α-hydroxylase	D12S90	0.737	1 (166 bp)	175	33.4	100	87	0.9	0.343
			4 (172 bp)	52	9.9	45	36	1.0	0.317
			6 (176 bp)	186	35.5	112	128	1.1	0.294
			7 (178 bp)	49	9.4	46	40	0.4	0.527
	D12S355	0.777	3 (176 bp)	25	4.8	18	28	2.2	0.138
			9 (184 bp)	102	19.6	61	90	5.6	0.018
			10 (186 bp)	220	42.3	143	102	6.9	0.009
			11 (188 bp)	72	13.8	62	58	0.1	0.752
	D12S83	0.782	3 (89 bp)	87	16.9	55	62	0.4	0.527
			5 (93 bp)	75	14.6	51	71	3.3	0.069
			6 (95 bp)	62	12.1	50	44	0.4	0.527
			7 (97 bp)	194	37.7	118	96	2.3	0.129

N = number of times the allele is seen in the parents; % Freq = the percent frequency of the allele; TR = number of times the allele was transmitted through either parent; NT = number of times the allele was not transmitted through either parent; H = heterozygosity of the marker based on the genotype of the parents.

two-point analysis of the three microsatellites showed a maximum lod score of 0.0 and multipoint analysis of the 1α-hydroxylase locus clearly excluded the significant contribution of this region to MS susceptibility with a lod score of less than −2.00 at a λ value of 1.335.

Our data do not support a role for the VDR, the DBP, or the 1α-hydroxylase genes in the susceptibility of MS in Canadians, although genetic heterogeneity or complexity among the MS families may have limited the ability of this study to detect linkage or association. Although we have excluded three prime candidate genes in the vitamin D pathway, other vitamin D related candidate genes may contribute to MS susceptibility. An environmental factor that influences risk and susceptibility to MS may still operate via a vitamin D mechanism.

Table 2 *Two-point linkage analysis of vitamin D loci at lambda value of 1.75*

Locus	Marker	IBD	Non-IBD	χ^2	mlod
VDR	D12S85	100	97	0.05	0.01
	*Taq*I	56	48	0.62	0.10
	*Apa*I	60	43	2.81	0.54
DBP	*Hae*III	40	44	0.19	0.00
	*Sty*I	38	47	0.95	0.00
1α-hydroxylase	D12S355	122	126	0.06	0.00
	D12S90	99	132	4.71	0.00
	D12S83	94	124	4.13	0.00

IBD = identical-by-descent from parent; non-IBD = non-identical-by-descent from parent.

Acknowledgment

The authors acknowledge the help of the following research assistants and MS clinic research nurses who were responsible for the collection of accurate clinical data: D. Bucciarelli; M. Van deVen; L. Mashal; T. Canero; E. Epstein; S. Christian; J. Boyle; J. Smith; L. Morrison; M. Hader; D. Heiser; B. Davis; M. Perera; P. Gaudet; C. Edgar; D. Slavik; J. Haynes; R. Julien-Bimm; K. Stevenson; M. Lemieux; P. Provencher; R. Arnaoutelis; C. Masse; F. Gosselin; M. Morash; P. Weldon; G. Alcock; K. Turpin; V. McBride; P. Fleming; and A. Pietromonaco.

Appendix

The Canadian Collaborative Study Group: S. Hashimoto, D. Paty, J. Oger, W. Hader, G. Rice, L. Metz, S. Warren, T. Auty, A. Nath, R. Nelson, D. Brunet, P. O'Connor, R. Paulseth, G. Francis, P. Duquette, J.-P. Bouchard, T. J. Murray, W. Pryse-Phillips, C. Powers, and Y. Lapierre.

References

1. Sadovnick AD, Ebers GC. Genetics of multiple sclerosis. Mult Scler 1995;13:99–118.
2. Goldberg P. Multiple sclerosis: vitamin D and calcium as environ-

mental determinants of prevalence (a viewpoint). Part 2: Biochemical and genetic factors. Int J Environ Studies 1974;6:19–27.
3. Nieves J, Cosman F, Hebert J, Shen V, Lindsay R. High prevalence of vitamin D deficiency and reduced bone mass in multiple sclerosis. Neurology 1994;44:1687–1692.
4. Cantorna MT, Hayes CE, DeLuca HF. 1,25-Didydroxyvitamin D3 reversibly blocks the progression of relapsing encephalomyelitis, a model of multiple sclerosis. Proc Natl Acad Sci 1996;93:7861–7864.
5. Hayes CE, Cantorna MT, DeLuca HF. Vitamin D and multiple sclerosis. Proc Soc Exp Biol Med 1997;216:21–27.
6. Ebers GC, Sadovnick AD, Risch NJ, et al. A genetic basis for familial aggregation in multiple sclerosis. Nature 1995;377:150–151.
7. Arnason A, Jensson O, Skaftadottir I, Birgisdottir B, Gudmundsson G, Johannesson G. HLA types, GC protein and other genetic markers in multiple sclerosis and two other neurological diseases in Iceland. Acta Neurol Scand 1980;62(suppl 78):39–40. Abstract.
8. The marker position on the chromosome 12 genetic map was identified at the Whitehead Institute for Biomedical Research website (http://carbon.wi.mit.edu:8000/cgi-bin/contig/sts_info/).

Anti-inflammatory drugs and Alzheimer-type pathology in aging

Article abstract—Anti-inflammatory drugs have been suggested as a treatment for AD. The authors examined the AD-type pathology in postmortem brain tissue from elderly nondemented individuals who were chronically exposed to anti-inflammatory drugs. The results suggest that 1) these drugs do not affect the formation of either senile plaques or neurofibrillary tangles and 2) nonsteroidal anti-inflammatory drugs may be more effective than steroids in treating AD because of their ability to suppress the microglial activation associated with senile plaques. **Key words:** AD—Senile plaques—Inflammation—Microglia—Anti-inflammatory drugs—Steroids—Nonsteroidal anti-inflammatory drugs.

NEUROLOGY 2000;54:732–734

Ian R.A. Mackenzie, MD

The concept that anti-inflammatory therapy may be useful in the treatment of AD is based on epidemiologic studies showing a decreased risk of AD in patients exposed to anti-inflammatory drugs[1] and from the demonstration of markers of inflammation in AD brain tissue.[2] Although the precise role of inflammation in AD pathogenesis is not known, the association of immune system proteins and immune-competent microglial cells with senile plaques (SP) suggests that inflammation may play a role in the development of SP[3]—a process believed to be of central importance in AD. Alternatively, pre-established SP may attract microglia and stimulate them to produce various proinflammatory mediators, thus helping to sustain and propagate the inflammatory process. In either case, activated microglial cells are capable of secreting a variety of potentially neurotoxic substances that could contribute to neurodegeneration in AD.[2] Although it seems reasonable to postulate that anti-inflammatory therapy could be of benefit by modifying these processes in AD, few published studies have examined the effect of these agents on either SP formation or the inflammation associated with SP.

In a previously reported study, we examined postmortem brain tissue from nondemented individuals with a history of long-term nonsteroidal anti-inflammatory drug (NSAID) use.[4] We found that although the degree of age-related SP and neurofibrillary tangle (NFT) pathology was similar to controls, tissue from NSAID users had significantly fewer activated microglial cells associated with SP.

We have subsequently extended these studies to include an evaluation of the effect of chronic glucocorticoid (steroid) use on AD-type pathology in aging. There are several reasons to study steroids specifically. Steroids have a more potent anti-inflammatory/immunosuppressant effect than NSAIDs and have proved to be useful in treating a variety of inflammatory neurologic conditions. Steroids may be able to suppress microglial proliferation, activation, and neurotoxin production.[5,6] Finally, a multicenter prospective clinical trial of treating AD with prednisone is currently underway.[7]

As in our previous study, we chose to focus on nondemented elderly individuals because they are at risk for developing AD and would be the preferred target for preventive therapy. Importantly,

From the Department of Pathology and Laboratory Medicine, Vancouver General Hospital and the University of British Columbia, Vancouver, BC, Canada.

Supported by a grant from the Alzheimer Society of Canada.

Received September 1, 1999. Accepted in final form October 19, 1999.

Address correspondence and reprint requests to Dr. Ian R.A. Mackenzie, Department of Pathology and Laboratory Medicine, Section of Neuropathology, Vancouver General Hospital, 855 West 12th Avenue, Vancouver, BC, Canada V5Z 1M9; e-mail: imackenz@vanhosp.bc.ca

See also page 588

 Copyright © 2000 by the American Academy of Neurology

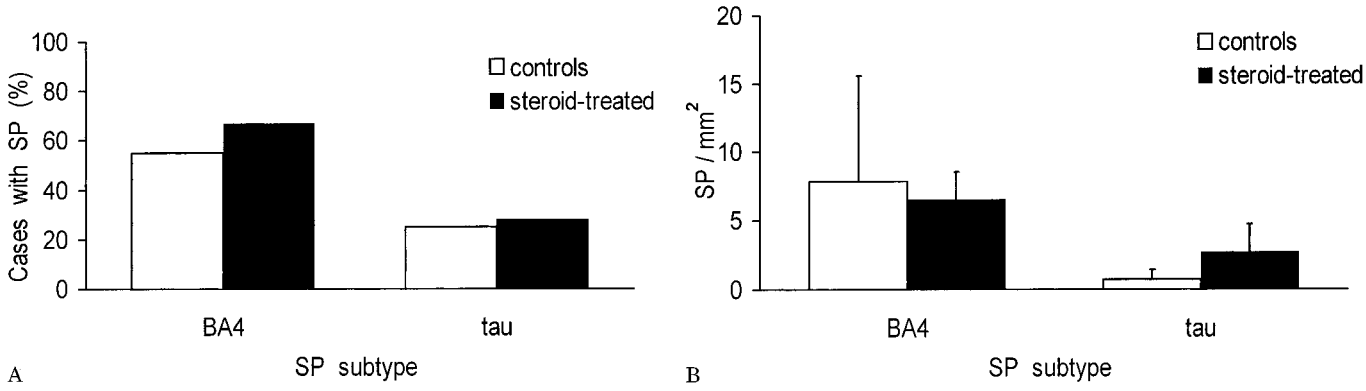

Figure 1. Patients treated with steroids did not differ from controls in either (A) the proportion of cases with senile plaques (SP) or (B) the mean number of SP. A, χ^2 analysis; B, ANOVA ± SEM.

SP associated with markers of inflammation similar to those in AD are often found in this group (so-called "pathologic aging").[3] Although a study of AD patients treated with steroids would have more direct relevance, pathologic material from a sufficient numbers of such cases is not currently available.

Methods. Autopsy reports, hospital medical records, and outpatient clinic charts were reviewed to identify patients fulfilling the following criteria: 1) a well-documented history of oral steroid use, for a minimum of 1 continuous year before death, with the final dose given within 48 hours of death; 2) no clinical history or pathologic evidence of neurologic disease, including dementia; and 3) age at death ≥60 years. Patients were excluded if they had been taking other anti-inflammatory, immunosuppressant, or antirheumatologic drugs. The final study group consisted of 18 patients (mean age, 73 ± 8 years), most of whom had rheumatoid arthritis. Four patients were taking steroids for other conditions including polyarteritis nodosa, chronic obstructive pulmonary disease, adrenal insufficiency, and polymyositis. All patients were receiving oral prednisone, in doses ranging from 5 mg to 40 mg per day; the dose often varied over the treatment period, being adjusted according to the individual's symptoms and side effects. Neurologically normal age-matched controls were selected to exclude those with a history of anti-inflammatory or immunosuppressant drug use or any medical condition likely to promote the frequent use of such drugs (n = 20; mean age, 74 ± 6 years). Because the inheritance of different *APOE* alleles is recognized as having a strong influence on the presence and number of SP, we confirmed that the two study groups were similar by performing *APOE* genotyping, using previously described methods[4] (no significant difference, ANOVA; data not shown).

Immunohistochemistry was performed on 4-μm–thick paraffin sections of formalin-fixed tissue from the mesial temporal lobe. Primary antibodies against βA4 protein (DAKO Beta-Amyloid, Glostrup, Denmark; formic acid pretreatment, 1:100 overnight) and tau (Sigma TAU-2, St. Louis, MO; 1:1000 for 1 hour) were used to demonstrate diffuse and neuritic SP. Neurofibrillary pathology was also assessed on the tau-immunostained sections. Activated microglia were identified using an anti–major histocompatibility complex II antibody (DAKO CR3/43; microwave antigen retrieval, 1:100 for 1 hour). Standard avidin-biotin complex techniques (Vectastain Elite Kit, Vector Laboratories, Burlingame, CA) were employed and the reactions were developed with diaminobenzidine (DAB).

The *prevalence* of different SP subtypes was determined by assessing βA4 and tau-immunostained sections for the presence of *any* SP. The *mean number* (areal density) of each type of SP was obtained by counting 10 adjacent, nonoverlap-

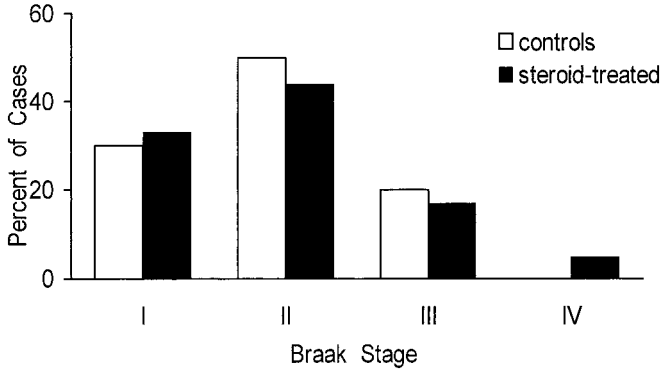

Figure 2. Steroid-treated patients and control subjects showed a similar degree of neurofibrillary pathology [ANOVA]. No case in either group was stage V or VI.

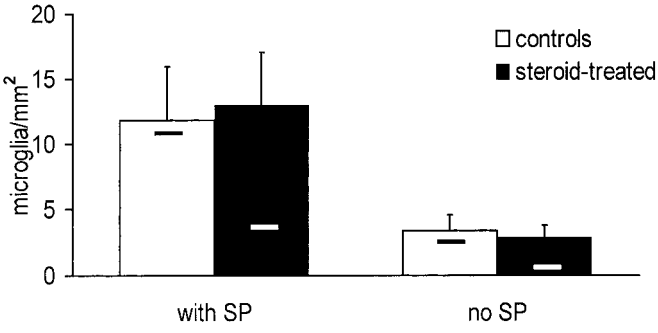

Figure 3. Steroid-treated patients and controls had similar numbers of activated microglial cells. Multiple regression analysis with patient age, the presence of senile plaques (SP), and steroid use as independent variables, ± SEM. Solid bars indicate mean values for corresponding groups of nonsteroidal anti-inflammatory drug (NSAID)–treated patients and no-NSAID controls; data from previous study.[4]

ping, 0.5-mm–wide strips of neocortex in the lateral wall of the collateral sulcus. The same method was used to quantify CR3/43+ activated microglia. The degree of neurofibrillary pathology was evaluated on tau-immunostained sections, according to the Braak staging method.

Results. There was no significant difference between the steroid-treated and control groups in either the prevalence or mean number of different SP subtypes (χ^2 analysis and ANOVA, respectively) (figure 1). The greater density of neuritic SP in the steroid-treated group was almost entirely the effect of a single patient who had a maximum of eight neuritic SP per square millimeter; the difference between the groups was not significant. The degree of neurofibrillary pathology was also similar between the two groups (ANOVA) (figure 2). Multiple regression analysis showed that both patient age and the presence of SP correlated positively with the number of CR3/43+ microglia ($p < 0.05$). Unlike the results from our previous study of NSAID exposure, a history of steroid use was *not* associated with any significant difference in the number of activated microglial cells; this was true when all cases were used in the analysis and when only those with SP were considered (figure 3).

Discussion. The epidemiologic evidence for anti-inflammatory drugs protecting against AD is much stronger for NSAIDs than for steroids.[1] Although all four of the studies that have examined steroid use as a risk factor for AD found an OR < 1 (indicating a protective effect), only the twin study of Breitner et al. had a result that was significant.[8] The fact that the ORs obtained in studies of NSAID use are more impressive than those for steroids does not necessarily mean that NSAIDs provide better protection against AD; the NSAID studies have generally included many more subjects, increasing the statistical strength. However, the results of our two studies provide an alternative explanation for the difference; NSAIDs may be more beneficial in preventing AD by virtue of their superior ability to suppress the specific type of inflammation that occurs in AD brain tissue.

There are other reasons why steroid treatment might be unsuitable for AD. Elevated serum cortisol may be associated with memory deficits and hippocampal atrophy.[9] Steroids can injure or kill hippocampal neurons by reducing their ability to withstand various types of metabolic insults, including the toxic effects of βA4 protein.[10] Finally, the systemic side effects of long-term steroid use make them unsuitable for treating AD patients, many of whom are prone to infection and fractures.

Acknowledgment

The author acknowledges the technical expertise of Caron Fournier, who performed the immunohistochemistry, and Dr. S. Chakrabarti, who conducted the *APOE* genotyping.

References

1. McGeer PL, Schulzer M, McGeer EG. Arthritis and anti-inflammatory agents as possible protective factors for Alzheimer's disease: a review of 17 epidemiologic studies. Neurology 1996;47:425–432.
2. McGeer PL, McGeer EG. The inflammatory response system of brain: implications for therapy of Alzheimer and other neurodegenerative diseases. Brain Res Rev 1995;21:195–218.
3. Mackenzie IRA, Hao C, Munoz DG. The role of microglia in senile plaque formation. Neurobiol Aging 1995;16:797–804.
4. Mackenzie IRA, Munoz DG. Nonsteroidal anti-inflammatory drug use and Alzheimer-type pathology in aging. Neurology 1998;50:986–990.
5. Colton CA, Chernyshev ON. Inhibition of microglial superoxide anion production by isoproterenol and dexamethasone. Neurochem Int 1996;29:43–53.
6. Ganter S, Northoff H, Mannel D, Gebicke-Harter PJ. Growth control of cultured microglia. J Neurosci Res 1992;33:218–230.
7. Aisen P, Altstiel L, Marin D, Davis K. Treatment of Alzheimer's disease with prednisone: results of pilot study and design of multicenter trial. J Am Geriatric Soc 1995;43:SA27. Abstract.
8. Breitner JCS, Welsh KA, Helms MJ, et al. Inverse association of anti-inflammatory treatments and Alzheimer's disease: initial results of a co-twin control study. Neurology 1994;44:227–232.
9. Starkman MN, Gerbarski SS, Bernet S, Schteingart DE. Hippocampal formation volume, memory dysfunction and cortisol levels in patients with Cushing's syndrome. Biol Psychiatry 1992;32:756–765.
10. Behl C, Lezoualch F, Trapp T, Widmann M, Skutella T, Holsboer F. Glucocorticoids enhance oxidative stress-induced cell death in hippocampal neurons in vitro. Endocrinology 1997;138:101–106.

Cerebrospinal fluid pyruvate levels in Alzheimer's disease and vascular dementia

Article abstract—Increased amounts of CSF pyruvate and lactate were found in patients with AD and patients with vascular dementia (VaD). In the AD group, CSF pyruvate values did not show any overlap with those obtained in controls; within the VaD group, the highest values were observed in possible VaD cases. A significant correlation between the severity of dementia and these biochemical parameters was also observed in both AD and possible VaD. The similarities of CSF pyruvate patterns observed in AD and possible VaD patients implicate a neurodegenerative component in this VaD subgroup. **Key words:** Pyruvate—Lactate—CSF—AD—Vascular dementia.

NEUROLOGY 2000;54:735–737

Lucilla Parnetti, MD, PhD; GianPaolo Reboldi, MD, PhD; and Virgilio Gallai, MD

It is well known that free radical–induced oxidative damage leads to reduced functional capacity of mitochondria in the aging brain.[1] Such a dysfunction, involving a decrease in glucose turnover and a decline in oxidative phosphorylation, is believed to be involved in the pathogenesis of several neurodegenerative disorders, including AD.[2]

A reduction in the activity of some key mitochondrial enzymes, mainly pyruvate dehydrogenase complex (PDHC), likely forces the brain to use a less efficient glycolytic pathway for its energy requirements.

The impairment of energy metabolism is an early feature of AD, often preceding the clinical picture.[3] We previously found increased levels of pyruvate and lactate in CSF of patients with AD, with pyruvate levels and the degree of cognitive impairment being also significantly associated.[4] With the aim of better evaluating the actual role of CSF pyruvate and lactate levels as biologic markers of AD, we performed these measurements in a larger group of AD patients and controls, extending the study to patients suffering from vascular dementia (VaD), which represents the second leading cause of dementia.

Patients and methods. The study population comprised 114 subjects. The control group consisted of 44 subjects (69 ± 10 years of age, mean ± SD). The AD group comprised 41 patients (71 ± 7 years of age), fulfilling the National Institute of Neurological and Communicative Disorders and Stroke–Alzheimer's Disease and Related Disorders Association (NINCDS-ADRDA) criteria[5] for probable AD. Twenty-nine VaD patients (70 ± 9 years of age) were also included. Values given are mean ± SD. According to National Institute of Neurological Disorders and Stroke–Association Internationale pour le Recherche et l'Enseignement en Neurosciences (NINDS-AIREN) criteria,[6] 18 fulfilled the diagnostic criteria for probable VaD and 11 for possible VaD. In both controls and demented subjects, lumbar punctures were performed in the morning, after overnight bed rest. CSF samples (15 mL) were divided into 1-mL aliquots and quickly stored at −80 °C until analyzed. CSF lactate and pyruvate concentrations were measured by enzymatic assay after deproteinization by adding 1 mL of 8% $HClO_4$ and centrifuging at 12,000 rpm for 10 minutes. All the procedures were performed in ice. Results are presented as mean ± SD. For biochemical variables, differences among groups were assessed by analysis of variance with the Bonferroni correction for multiple comparisons. Differences in clinical scores were analyzed by the Kruskal-Wallis test. Correlation between clinical and biochemical variables was assessed by the Spearman rank correlation coefficient.

Results. As reported in the table, both AD and VaD patients show significantly lower Mini-Mental State Examination (MMSE) score values than the controls, yet AD and VaD groups do not differ from each other. CSF pyruvate levels appear significantly higher in AD and VaD subjects as compared with controls. Notably, pyruvate levels in AD (range 5.8 to 16.2) do not overlap with those found in controls (range 1.0 to 3.3). CSF lactate levels are higher in AD as compared with both VaD and controls. These two latter groups do not differ from each other. However, when subgrouping VaD according to NINDS-AIREN criteria, possible VaD shows higher CSF-lactate levels than controls (111 ± 27 versus 85 ± 19; $p < 0.001$), whereas probable VaD patients (76 ± 16) are similar to controls (85 ± 19; p = not significant [NS]) and lower than AD (108 ± 21; $p < 0.001$). The same holds true for CSF pyruvate: possible VaD shows levels (7 ± 2.5) higher than controls (2 ± 0.6; $p < 0.001$), whereas probable VaD does not (2.8 ± 1.1; p = NS).

Correlation analysis between clinical and biochemical parameters shows a significant association between the severity of dementia (as assessed by MMSE scores) and CSF pyruvate levels in the whole group of demented patients ($r_s = -0.57$, $p < 0.0001$), and specifically in AD ($r_s = -0.81$, $p < 0.001$) and possible VaD ($r_s = -0.92$, $p < 0.0001$) groups, whereas in probable VaD ($r_s = -0.31$, p = NS), no strong correlation is evident (figure A). A similar correlation pattern is present for CSF lactate levels (see figure B) in the whole group ($r_s = -0.55$, $p < 0.001$) and within subgroups (AD $r_s = -0.69$, $p < 0.001$; possible VaD $r_s = -0.67$, $p < 0.02$; probable VaD $r_s = -0.48$, p = NS).

From the Institute of Nervous and Mental Diseases (Drs. Parnetti and Gallai), and the Department of Internal Medicine (Dr. Reboldi), University of Perugia, Perugia, Italy.

Received May 26, 1999. Accepted in final form October 1, 1999.

Address correspondence and reprint requests to Dr. Lucilla Parnetti, MD, PhD, Institute of Mental and Nervous Diseases, Via Enrico dal Pozzo, 06126 Perugia, Italy; e-mail: parnetti@unipg.it

Copyright © 2000 by the American Academy of Neurology

Table *Age, MMSE score, and CSF lactate and pyruvate levels in subjects with AD, VaD, and control subjects*

Characteristic	Control subjects	AD	VaD	*p* Value
Number of subjects	44	41	29	
Age, y	69 ± 10	71 ± 7	70 ± 9	NS (ANOVA)
MMSE score	28 ± 1.5	15 ± 6.7*	16 ± 6.7*	<0.001 (Kruskal-Wallis test)
CSF lactate (mg/L)	85 ± 19	108 ± 21*	90 ± 27†	<0.0001 (ANOVA)
CSF pyruvate (mg/L)	2 ± 0.6	10 ± 2.9*	4.5 ± 2.7*†	<0.0001 (ANOVA)

Values are means ± SD.

Lactate and pyruvate multiple comparisons (Bonferroni method): * $p < 0.001$ (AD or VaD) versus control subjects; † $p < 0.001$ AD versus VaD.

MMSE = Mini-Mental State Examination; VaD = vascular dementia; ANOVA = analysis of variance.

Discussion. Increased amounts of pyruvate levels in CSF of patients with AD were found without any overlap with the values observed in control subjects. Furthermore, CSF pyruvate levels were significantly associated with the degree of cognitive impairment, thus confirming a previous report on a small group of patients.[4] A similar pattern was observed for CSF lactate. These data might be interpreted as the result of mitochondrial functional impairment taking place in AD, where pyruvate dehydrogenase complex has been shown to be altered both in experimental animals and in cell cultures.[7] This would imply that metabolic substrates, e.g., pyruvate and lactate, are not properly used in the oxidative phosphorylation cycle and, therefore, accumulate. The behavior of pyruvate and lactate values observed in the two VaD subgroups is worth noting. In fact, patients with possible VaD show concentrations of both metabolites quite similar to those observed in patients with AD, whereas probable (i.e., "pure") VaD does not differ from the control group. This finding is in keeping with the pathophysiologic bases of possible VaD, where the coexistence of both neurodegenerative and vascular pathologies can be assumed. Victoroff et al.[8] found pathologic changes of AD in 55% of patients clinically diagnosed with VaD. Although this study was conducted before the publication of the NINDS-AIREN criteria for possible and probable VaD, it is reasonable to assume that the Alzheimer component is more likely present in the "mixed" cases (i.e., possible VaD) rather than in the "pure" (i.e., probable) VaD subgroup. In this context, high CSF levels of pyruvate in both AD and possible VaD favor the hypothesis of a wide overlap between AD and VaD, where the vascular component might represent a factor precipitating or anticipating a preclinical AD.[9]

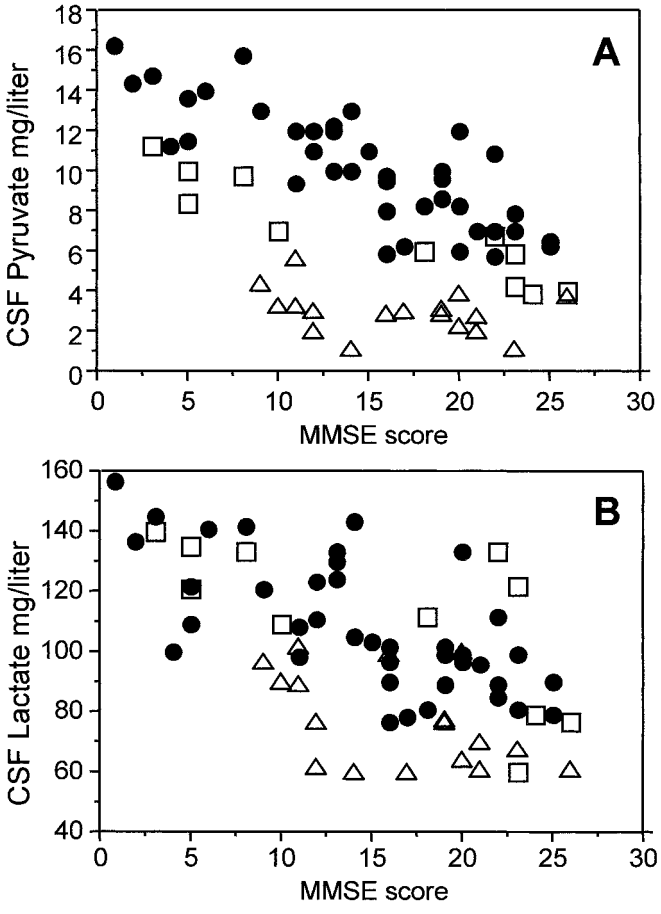

Figure. Correlation analysis between CSF pyruvate levels and Mini-Mental State Examination (MMSE) scores (A) and CSF lactate values and MMSE scores (B) in AD and possible and probable vascular dementia (VaD). ●, AD; □, possible VaD; △, probable VaD.

References

1. Beal MF. Aging, energy and oxidative stress in neurodegenerative diseases. Ann Neurol 1995;38:357–366.
2. Parker WD, Filley CM, Parks JK. Cytochrome oxidase deficiency in Alzheimer's disease. Neurology 1990;40:1302–1303.
3. Hoyer S. Oxidative energy metabolism in Alzheimer brain. Studies in early-onset cases. Mol Chem Neuropathol 1992;16: 207–224.
4. Parnetti L, Gaiti A, Polidori MC, et al. Increased cerebrospinal fluid pyruvate levels in Alzheimer's disease. Neurosci Lett 1995;199:231–233.
5. McKhann G, Drachman D, Folstein M, Katzman R, Price D, Stadlan EM. Clinical diagnosis of Alzheimer's disease: report of the NINCDS-ADRDA Work Group under the auspices of Department of Health and Human Service Task Force on Alzheimer's Disease. Neurology 1984;34:939–944.

6. Roman GC, Tatemichi TK, Erkinjuntti T, et al. Vascular dementia: Diagnostic criteria for research studies. Report of the NINDS-AIREN International workshop. Neurology 1993;43:250–260.
7. Blass JP, Gibson GE. Non-neural markers in Alzheimer's disease. Alzheimer Dis Assoc Disord 1993;6:205–224.
8. Victoroff J, Mack WJ, Lyness SA, et al. Multicenter clinicopathological correlation in dementia. Am J Psychiatry 1995;152:1476–1484.
9. Pasquier F, Leys D. Why are stroke patients prone to develop dementia? J Neurol 1997;244:939–944.

Amnesic syndrome with bilateral mesial temporal lobe involvement in Hashimoto's encephalopathy

Article abstract—A 25-year-old woman presented with a subacute confusional state, headaches, unsteadiness, myoclonus, seizures, and an amnesic syndrome as a manifestation of Hashimoto's encephalopathy. Investigations showed biochemical hypothyroidism, raised thyroid microsomal antibodies, and weakly positive antineuronal antibodies. A T2-weighted MRI of the brain showed bilateral symmetric areas of increased signal in the mesial temporal lobes and hippocampi that had a low signal intensity on T1-weighted imaging. Despite clinical and radiologic improvement after steroid and thyroid hormone replacement therapy, a severe amnesic syndrome with associated localized MRI abnormalities persists. **Key words:** Hashimoto's encephalopathy—Amnesic syndrome—MRI.

NEUROLOGY 2000;54:737–739

Dominick J.H. McCabe, MRCPI; Teresa Burke, PhD; Sean Connolly, MD; and Michael Hutchinson, FRCP

Hashimoto's encephalopathy was first described in 1966[1] and may present with a subacute or acute encephalopathic process, seizures and "stroke-like" episodes, often in association with myoclonus and tremulousness.[2,3] The disorder usually responds to steroids, and although an 80% remission rate has been reported,[4] frequent relapses are not uncommon,[2,3] with some patients having significant residual disability.

Case history. A 25-year-old left-handed nurse had a 7-week history of headaches, nausea, increasing unsteadiness and tremulousness, and a 2-week history of feeling cold with reduced appetite before admission. She began behaving inappropriately at work and her colleagues noticed that she was unable to make a bed. She had one episode of left hand weakness and expressive dysphasia for 30 minutes, and subsequently a 10 minute episode of left facial drooping. Assessment at her local hospital at that stage showed a normal neurologic examination, a normal brain CT, and a CSF protein of 0.64 g/L. Seven weeks after the onset of symptoms, she developed generalized status epilepticus, treated with IV phenytoin and, later, general anesthesia. Two days later, the patient was transferred to our hospital for assessment. General examination was normal with no palpable goiter. Verbal responses were slow, and cognitive assessment showed disorientation in time, place, and person, with normal verbal and visual registration, but an inability to recall any of four objects at 10 minutes, or reproduce a crossed-flags figure previously drawn correctly. There was a severe anterograde amnesia, and a significant retrograde amnesia for at least 6 months prior to presentation. The remainder of the cognitive and neurologic examination was normal.

Thyroid stimulating hormone (TSH) was markedly increased at greater than 100 mU/L (normal range = 0.49–4.67) and free T_4 was reduced at 6.1 pmol/L (normal range = 9.1–23.8). The thyroid antimicrosomal antibody titer was 1/25,600 but antithyroglobulin antibodies were negative. Antineuronal antibodies were positive at a titer of 1/50-1/100, and antinuclear antibody titers were 1/100, but antibodies to DsDNA, Sm, RNP, Ro, La, Scl-70 and Jo-1 were negative, with a normal serum angiotensin converting enzyme (ACE) level and toxicology profile. A T2-weighted MRI scan of brain showed bilateral symmetric areas of high signal intensity involving the mesial and anterior temporal lobes and hippocampi (figure 1). The lesions were of low signal intensity on the T1-weighted MRI images, with some associated localized swelling of the mesial temporal lobes (figure 2). Repeat CSF examination showed a protein of 0.52 g/L, but was otherwise normal in all respects with negative oligoclonal bands and a negative CSF PCR for herpes simplex virus (HSV). The initial scalp EEG showed symmetric slowing of the rhythmic background activity to 6 per second, with generalized discharges of theta and delta slowing without either focal or epileptiform abnormalities.

A diagnosis of Hashimoto's encephalopathy with hypothyroidism was made, and the patient was treated with 1 g of IV methylprednisolone daily for 5 days, followed by 60 mg daily of oral prednisolone. In addition, 10 mg of IV triiodothyronine four hourly and 50 μg daily of oral levo-

From the Department of Neurology (Drs. McCabe, Connolly, and Hutchinson), St. Vincent's Hospital, Elm Park, Dublin; and the Department of Psychology (Dr. Burke), University College Dublin, Belfield, Dublin, Ireland.

D.J.H.M.'s research is funded by a grant from the NHS Research and Development Programme in the UK and a grant from the Brain Research Trust.

Received July 13, 1999. Accepted in final form November 1, 1999.

Address correspondence and reprint requests to Dr. Dominick J.H. McCabe, Department of Clinical Neurology, Institute of Neurology, University College London, The National Hospital for Neurology and Neurosurgery, Queen Square, London WC1N 3BG, UK; e-mail: d.mccabe@ion.ucl.ac.uk

Copyright © 2000 by the American Academy of Neurology

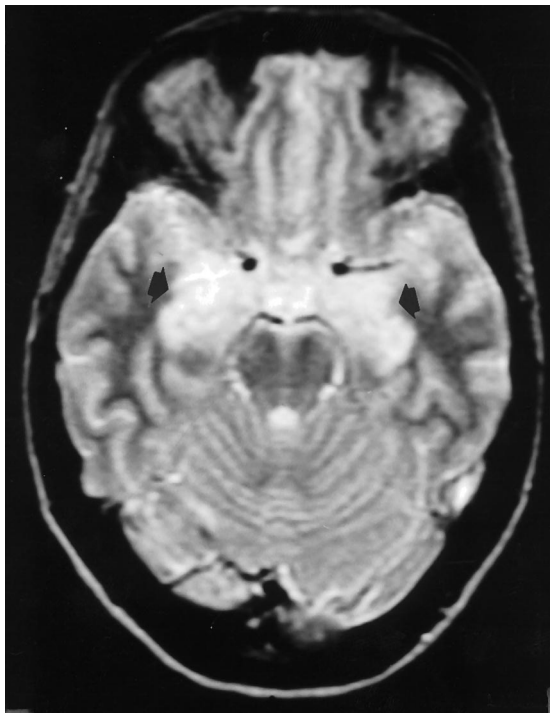

Figure 1. Axial T2-weighted MRI brain scan through the temporal lobes shows bilateral areas of increased signal intensity involving the mesial temporal lobes and hippocampi (arrows).

thyroxine were given, and a 14 day course of 10 mg/kg of IV acyclovir eight hourly was begun while awaiting the PCR result for HSV.

Two days after admission, she developed complex partial seizure activity, followed again by secondary generalized tonic status epilepticus, necessitating ventilation and general anesthesia. Another scalp EEG performed 2 hours after control of clinical status showed focal theta and delta activity in the right temporal region, with no evidence of organized seizure activity. The patient became more alert and responsive during the remainder of her inpatient stay and remained seizure free. A repeat MRI of the brain one week after commencing steroid therapy showed a reduction in the extent of the high signal lesions in the mesial temporal lobes on the T2-weighted images, and the lesions did not enhance with gadolinium on T1-weighted imaging. At this stage, there was some degree of atrophy of the left anterior temporal lobes, which was more marked on the right than on the left.

Figure 2. Sagittal T1-weighted MRI brain (without gadolinium) demonstrates a low signal intensity lesion, with localized swelling of the right mesial temporal lobe (arrow).

The patient was discharged after two and a half weeks on a reducing dose of prednisolone (40 mg daily, decreasing to 10 mg daily after six months), and levothyroxine 50 to 100 μg daily.

She had four self-limiting simple partial seizures over the following 6 months, and although more independent, she has been unable to return to work because of her amnesic state. Neuropsychologic assessment 6 months after discharge showed impaired learning on both verbal and nonverbal recurring sequence tests, and particular difficulty with delayed recall of both verbal and visual material, as assessed by the Wechsler Memory Scale-Revised test.[5] In addition, recognition of words was impaired (<5th percentile) on the Warrington Recognition Memory Test (RMT),[6] but recognition memory for faces remained intact, as evidenced by adequate performance on both the Warrington RMT and the Mooney Face Recognition Test.[7] There was no evidence of significant deterioration of general intellectual ability, or of impairment of attention, concentration, verbal fluency, or information processing speed.

Discussion. The clinical and laboratory features in this case support a diagnosis of Hashimoto's encephalopathy, with a significant residual amnesic state, despite treatment with steroids. Severe anterograde amnesia is usually secondary to bilateral lesions of the hippocampus, amygdala or their projections, or a lesion involving the septal region, mamillary bodies, mamillothalamic tracts, anterior and dorsomedial nuclei of the thalamus, cingulate gyrus, or cingulum.[8] The marked bilateral hippocampal and mesial temporal lobe changes on the MRI account for the amnesic state in this case, and explain the disturbance in both verbal and nonverbal memory. Although memory impairment has been reported in Hashimoto's encephalopathy,[2-4] a severe amnesic syndrome with similar anatomically localized MRI abnormalities has not been previously described.

Descriptions of MRI changes in Hashimoto's encephalopathy are few, and include normal images,[4] diffuse[3,4] or focal[4] white matter abnormalities (that may be reversible),[3] and generalized atrophy.[3] Takahashi et al. described a 12-year-old girl with Hashimoto's encephalopathy in association with multiorgan autoimmune dysfunction, who had similar bilateral hippocampal high signal lesions on T2-weighted MRI imaging.[9] The lesions were isointense on the T1-weighted images in their patient in contrast to the hypointense T1-weighted lesions seen in this case.

The marked symmetry and nonhemorrhagic nature of the lesions, in addition to the normal CSF white cell count and negative PCR test for HSV,

argue against an etiologic role for herpes simplex virus in this situation. The clinical course and the absence of any other symptoms, signs or markers of malignancy do not support a diagnosis of paraneoplastic limbic encephalitis, which can produce similar MRI findings. The MRI changes are not believed to be secondary to prolonged nonconvulsive status epilepticus, despite the fact that the scalp EEG may occasionally fail to show discrete epileptiform activity and is less sensitive than depth electrode recording in diagnosing nonconvulsive complex partial status epilepticus.[10] However, although nonconvulsive complex partial status epilepticus may be associated with transient focal abnormalities on neuroimaging,[10] one would not expect bilateral symmetric MRI involvement with subsequent early anterior temporal lobe atrophy as a consequence of ictal activity.

The pathogenesis of the encephalopathy associated with Hashimoto's thyroiditis is not fully understood, but several theories have been proposed. These include an autoimmune cerebral vasculitis, with or without immune complex deposition,[2,4] and an antineuronal antibody mediated mechanism.[4,9] Cerebral vasculitis may produce multifocal and bilateral MRI changes, but this mechanism is unlikely to cause such localized and symmetric radiologic abnormalities as seen in this case. Although weakly positive (titers of 1/50 to 1/100), this is the first report of antineuronal antibodies in the serum in Hashimoto's encephalopathy. Shaw et al.[2] suggested that there may be a shared, but as yet unidentified, antigen between the brain and the thyroid gland, and that it is possible that the same antibody is reactive against a common neuronal and thyroid antigen. The hyperintense T2-weighted MRI findings could theoretically be explained by the binding of circulating antineuronal antibodies to neuronal antigens, with a subsequent inflammatory response and resultant edema. The "antineuronal" theory is supported by the early development of temporal lobe atrophy that could arise because of rapid neuronal destruction and cell death. This mechanism has been alluded to previously,[9] but does not fully explain why the abnormalities were localized. Nevertheless, assays for antineuronal antibodies should be performed in patients with Hashimoto's encephalopathy to facilitate further study of their pathogenic significance.

Acknowledgment

The authors thank Professor Michael A. Farrell for performing the antineuronal antibody assays.

References

1. Brain L, Jellinek EH, Ball K. Hashimoto's disease and encephalopathy. Lancet 1966;2:512–514.
2. Shaw PJ, Walls TJ, Newman PK, Cleland PG, Cartlidge NEF. Hashimoto's encephalopathy: a steroid-responsive disorder associated with high anti-thyroid antibody titers—report of 5 cases. Neurology 1991;41:228–233.
3. Bohnen NILJ, Parnell KJ, Harper CM. Reversible MRI findings in a patient with Hashimoto's encephalopathy. Neurology 1997;49:246–247.
4. Kothbauer-Margreiter I, Sturzenegger M, Komor J, Baumgartner R, Hess CW. Encephalopathy associated with Hashimoto thyroiditis. J Neurol 1996;243:585–593.
5. Wechsler D. Wechsler Memory Scale-Revised. New York: The Psychological Corporation Harcourt Brace Jovanovich, 1987.
6. Warrington EK. Recognition Memory Test. Windsor, UK: NFER-Nelson, 1984.
7. Milner B. Visual recognition and recall after right-temporal lobe excision in man. Neuropsychologia 1968;6:191–209.
8. Brazis PW, Masdeu JC, Biller J The localization of lesions affecting the cerebral hemispheres: memory disturbances. In: Localization in Clinical Neurology, 3rd ed. Boston: Little, Brown, 1996:449–534.
9. Takahashi S, Mitamura R, Itoh Y, Suzuki N, Okuno A. Hashimoto encephalopathy: etiologic considerations. Pediatr Neurol 1994;11:328–331.
10. Shorvon SD. Clinical forms of status epilepticus. In: Shorvon SD, ed. Status epilepticus: its clinical features and treatment in children and adults. Cambridge: Cambridge University Press, 1994:34–138.

Frequency and duration of hospitalization of patients with AD based on Medicare data: CERAD XX

Article abstract—Medicare records on 477 Consortium to Establish a Registry for Alzheimer's Disease patients with AD for 1991 through 1995 showed a hospitalization rate of 0.37/person-year with a length of stay of 3.7 days/person-year (average of 10 days/hospitalization). Unmarried and less-educated patients with AD were admitted to the hospital more frequently, and, along with black patients, had a longer length of stay. Frequency and duration of hospitalization were greater in the patients with AD than in Medicare beneficiaries in general, but the rate of diagnostic/therapeutic procedures was lower. **Key words:** AD—Consortium to Establish a Registry for Alzheimer's Disease—Medicare—Hospitalization—Length of stay—Discharge diagnoses.

NEUROLOGY 2000;54:740–743

G. Fillenbaum, PhD; A. Heyman, MD; B. Peterson, PhD; C. Pieper, DrPH; and A.L. Weiman, MA

AD is a common progressive dementing disorder of the aged. Many of the published estimates of rate and duration of hospitalization in AD are imputed based on small numbers in geographically restricted areas. It generally is acknowledged that more accurate studies are needed[1-3] based on the experience of patients with well-defined diagnoses of this disorder. Here we present information on frequency and duration of hospitalization by demographic characteristics and reason for hospitalization in nationally distributed, clinically diagnosed patients with AD.

Methods. *Cases.* Of clinically diagnosed patients with AD enrolled between 1987 and 1995 at 24 major medical centers throughout the United States participating in the Consortium to Establish a Registry for Alzheimer's Disease (CERAD) program, 481 were 65 years of age or older in 1991 and had social security numbers potentially permitting linkage with Health Care Financing Administration (HCFA) data. Of these, a secure match was feasible for 477 (99%). They were linked with HCFA Medicare Provider Analysis and Review (MEDPAR) files for 1991 through 1995. Autopsies performed on 134 (51.9%) of the first 258 decedents in CERAD confirmed the diagnosis in 87%.

Number of hospital admissions and length of stay. The total number of hospital admissions per person-year from 1991 through 1995 was estimated as the total number of hospital admissions divided by the total duration of follow-up. For any given year, patients could contribute person-years to the denominator only if they were in the HCFA Denominator file for that year and were 65 years of age or older. Thus, a patient with AD who became 65 years of age on February 1, 1994, and died on November 30, 1994, would contribute 0.83 person-year to the denominator of the statistic. The same methods were used to estimate length of stay (LOS) in the hospital per person-year.

We calculated the CIs around our estimates of number of hospital admissions per person-year (LOS/person-year) by use of Generalized Estimating Equations as implemented by the SAS GENMOD procedure.[4] In particular, Poisson regression analysis with log link function and overdispersion scale parameter was used to model a subject's total number of hospital admissions (and, separately, LOS) during 1991 through 1995 as a function of each of the demographic variables (table 1). The logarithm of the number of years of follow-up was used as an "offset" (i.e., a regression variable with a constant coefficient of 1 for each observation). Predicted values from these models for offset = 0 (equivalent to 1 person-year) gave estimates identical to those described above, as well as upper and lower confidence bounds.

Analyses involving age took into account age change across time. Five separate dichotomous variables were created to indicate whether a patient was 75 years of age or older on January 1, 1991, 1992, ... 1995. A subject's number of hospital admissions (and LOS) and number of years of follow-up observation were calculated for each of the 5 years separately. Repeated measures Poisson regression analysis (with a maximum of five timepoints per subject) was used to regress the number of hospital stays in a year on age in January of the corresponding year. The logarithm of the number of years of follow-up was used as an offset. Predicted values at offset = 0 for each of the two age groups gave estimates of the number of hospital admissions (and LOS) per person-year.

Discharge diagnoses and surgical/diagnostic procedures. Although the 1991 through 1995 MEDPAR files contained codes for up to 10 diagnoses and up to 10 procedures for each patient record, we used only the first two diagnostic and first two procedure fields for our calculations, as nearly all patients had this number. If we had included a larger number of diagnoses (or procedures), we might have increased the influence of patients who were sicker and possibly with conditions of lesser relevance. We calculated the percentage of diagnoses and procedures that fell into preselected International Classification of Diseases (ICD)-9-CM categories. Only hospitalized patients were included in this analysis; patients with two diagnoses were included in the analysis twice.

Comparison with Medicare beneficiaries. Where feasible, we compared data from our patients with AD with

From the Center for the Study of Aging and Human Development (Drs. Fillenbaum and Weiman), the Division of Neurology (Dr. Heyman), and the Division of Biometry (Drs. Peterson and Pieper), Duke University, Durham, NC.

Supported in part by NIH grant #AG06790.

Received May 18, 1999. Accepted in final form October 1, 1999.

Address correspondence and reprint requests to Dr. Albert Heyman, Box 3203, Duke University Medical Center, Durham, NC 27710.

 Copyright © 2000 by the American Academy of Neurology

Table 1 *Number of admissions and length of stay per person-year (1991–1995) by demographic characteristics of Consortium to Establish a Registry for Alzheimer's Disease (CERAD) cases (n = 477), and number of hospital admissions per person-year (1992–1994) by demographic characteristics reported by Medicare Current Beneficiary Survey*

	No. of hospital admissions/person-year				Length of stay/person-year		
Characteristic	% CERAD	% MCBS	OR (95% CI)	*p* Value	MCBS	OR (95% CI)	*p* Value
Age at entry (CERAD)							
<75 y	53.7	60.1	0.34 (0.28, 0.41)	0.17	0.16*	3.2 (2.5, 4.1)	0.07
≥75 y	46.3	38.6	0.40 (0.34, 0.46)		0.23	4.3 (3.5, 5.4)	
Race							
White	13.0	82.8	0.35 (0.30, 0.41)	0.12	0.18	3.3 (2.7, 4.0)	0.001
Black	87.0	8.9	0.47 (0.34, 0.65)		0.21	6.5 (4.5, 9.4)	
Sex							
Men	43.4	43.2	0.40 (0.33, 0.50)	0.23	0.19	3.8 (2.9, 5.1)	0.82
Women	56.7	56.8	0.34 (0.28, 0.41)		0.18	3.7 (2.9, 4.7)	
Education†							
<12 y	31.8	41.4	0.47 (0.38, 0.58)	0.004		5.1 (3.9, 6.7)	0.006
≥12 y	68.2	58.6	0.31 (0.26, 0.38)			3.1 (2.4, 3.9)	
Marital status‡							
Married	67.2	54.8	0.32 (0.27, 0.39)			3.0 (2.3, 3.8)	
Not married	32.8	45.2	0.45 (0.36, 0.56)	0.02		5.2 (4.0, 6.8)	0.003
Region							
Northeast	40.0		0.39 (0.32, 0.48)	0.64		4.6 (3.6, 5.9)	0.19
Midwest	25.8		0.35 (0.27, 0.47)			3.0 (2.0, 4.5)	
South	8.4		0.26 (0.12, 0.53)			2.9 (1.1, 7.1)	
West	25.8		0.35 (0.26, 0.46)			3.1 (2.1, 4.7)	
Overall			0.37 (0.32, 0.42)		0.18	3.7 (3.1, 4.5)	

Blank spaces under Medicare Current Beneficiary Survey (MCBS) indicate data unavailable for MCBS on website. % For MCBS may not total 100 because of categories not reported here.

* Data apply to noninstitutionalized. Data for total group not provided.
† Data missing for two CERAD cases.
‡ Data missing for one CERAD case.

published information for the years 1991 through 1995 on Medicare beneficiaries.

Results. The median length of follow-up for the 477 patients with AD was 4.2 years. Table 1 provides the person-year rate of hospitalization and LOS by patients' demographic characteristics. Between 1991 and 1995, 289 patients (61%) had been hospitalized for a total of 616 admissions, for which we considered 1,199 discharge diagnoses. They had 0.37 admission/person-year, with an average LOS of 3.7 days, or an average of 10 days/hospitalization (0.37/3.7). This compares with a rate for Medicare beneficiaries of 306/1,000 to 344/1,000 between 1991 and 1995, an average LOS/1,000 of 2.38 to 2.67 days, and an average LOS/hospitalization of 6.9 to 8.6 days.[5] The less-educated and unmarried patients had more hospitalizations and, together with black patients, had a longer LOS.

Among the 289 patients entering a hospital, 189 (65%) had one or more diagnostic, therapeutic, or surgical procedures. Procedures were reported for 286 (46.4%) of the hospitalizations, for which we considered 442 procedures. In contrast, procedures were reported for approximately 60% of hospitalizations of Medicare beneficiaries in the same interval.

Table 2 lists discharge diagnoses by ICD-9-CM categories. Direct comparison with HCFA discharge diagnostic data is not possible, as our data refer to those hospitalized, whereas HCFA data refer to rates per 1,000 enrollees. We therefore compared the rank-order of the medical classes for our patients with AD with the HCFA report for Medicare beneficiaries for calendar year 1993, the midpoint of 1991 through 1995.[6] Spearman's rho (0.37) indicates that our hospitalized patients with AD were discharged with diagnoses different from those of Medicare beneficiaries. In particular, our patients with AD had higher rates of endocrine, nutritional, metabolic, and immunity disorders, and, as expected, nonpsychotic mental disorders, dementias, and degenerative brain diseases. Diseases of the respiratory system were ranked second in each group, but neoplasms, ranked 6 for the Medicare beneficiaries, were ranked 11.5 (of 15) for the patients with AD.

Table 3 lists the ICD-9-CM codes for the first two diag-

Table 2 *Frequency (n) and % of first two discharge diagnoses by International Classification of Diseases (ICD)-9-CM classification, in descending rank order, for hospitalized AD cases (1991–1995), and discharge diagnosis/1,000 Medicare beneficiaries and rank order for the same ICD-9-CM classifications for 1993*

ICD-9-CM classification	Disease	Hospitalized AD cases		Medicare beneficiaries	
		n (%)	Rank	Discharge dx/ 1,000 enrollees	Rank
290–319, 330–337, 797	Nonpsychotic mental disorder, dementias, and degenerative brain disease	262 (21.9)	1	14	10.5
460–519	Diseases of respiratory system	169 (14.1)	2	38	2
240–279	Endocrine, nutritional, metabolic, and immunity disorders	139 (11.6)	3	13	12
410–429*	Heart disease (subset)	100 (8.3)	4.5	65	1
580–629	Diseases of genitourinary system	100 (8.3)	4.5	17	7.5
800–999	Injury and poisoning	88 (7.3)	6	25	4
520–579	Diseases of digestive system	84 (7.0)	7	32	3
780–799†	Ill-defined, nonspecific disorder	78 (6.5)	8	15	9
001–139	Infectious, parasitic disease	45 (3.8)	9	8	13
430–438*	Cerebrovascular disease (subset)	34 (2.8)	10	17	7.5
680–709	Diseases of skin, subcutaneous tissue	28 (2.3)	11.5	5	14
140–239	Neoplasms	28 (2.3)	11.5	21	6
	Other diagnoses, including V codes	18 (1.5)	13	24	5
710–739	Diseases of musculoskeletal system, connective tissue	14 (1.2)	14	14	10.5
280–289	Diseases of blood, blood-forming organs	12 (1.0)	15	3	15

* 410–429, 430–438 are subsets within 390–459: Diseases of the circulatory system.
† Excluding 797 for hospitalized AD cases, but including 797 for Medicare beneficiaries.

nostic/therapeutic procedures. Closer agreement with HCFA data is found for these (Spearman's rho = 0.81) than for discharge diagnoses.[6]

Discussion. Although our population sample is larger in size and better distributed geographically than those usually reported, these patients nevertheless represent those admitted to tertiary sites and thus may not be representative of patients with AD in general. Their demographic characteristics differ from those of the Medicare population in ways that have contrary effects on hospitalization and LOS.[7] Nevertheless, our findings agree with those reported

Table 3 *Frequency (n) and % of first two discharge-reported procedures by International Classification of Diseases (ICD)-9-CM classification in descending rank order for hospitalized AD cases (1991–1995), and procedure diagnosis/1,000 Medicare beneficiaries and rank order for the same ICD-9-CM classifications for 1993*

ICD-9-CM procedure codes	Disease	Hospitalized AD cases		Medicare beneficiaries	
		n (%)	Rank	Procedures/ 1,000 enrollees	Rank
87–99	Miscellaneous	182 (41.2)	1	54	1
42–54	Digestive system	95 (21.5)	2	35	2.5
76–84	Musculoskeletal system	49 (11.1)	3	22	4
85–86	Dermatologic system	23 (5.2)	4	7	6.5
55–59	Urinary system	19 (4.3)	5	6	8
35–39	Cardiovascular system	16 (3.6)	7	35	2.5
60–71	Genital organs	16 (3.6)	7	9	5
30–34	Respiratory system	16 (3.6)	7	7	6.5
08–16	Eye	10 (2.3)	9	1	11.5
01–05	Nervous system	9 (2.0)	10	4	9
18–29	Ear, nose, and throat	6 (1.4)	11	1	11.5
40–41	Hematologic/lymphatic system	1 (0.2)	12	2	10

in other uncontrolled analyses and show an increased frequency of hospitalization and LOS in patients with AD or cognitive impairment.[8-10] Contrary findings have also been reported.[3]

We found no studies reporting the reasons for hospitalization of patients with AD. Compared with all Medicare beneficiaries, our patients with AD had a higher rate of discharge diagnoses in the endocrine, nutritional, metabolic, and immunity disorders category. This could reflect improper or inadequate care of patients with AD. The lower frequency of neoplasms may, however, indicate a reluctance by medical practitioners to identify, in these patients, the presence of conditions that may require aggressive procedures. The lower rate of diagnostic, therapeutic, or surgical procedures in the patients with AD than in Medicare beneficiaries suggests less intervention, perhaps reflecting differences for hospital admission rather than disinclination to treat.

These data indicate increased frequency, longer stay, different reasons for hospitalization, and less-aggressive intervention in patients with AD than in the Medicare beneficiary population. They suggest that the cost of hospital care may differ, which is an issue now under review.

References

1. Ernst RL, Hay JW. Economic research on Alzheimer disease: a review of the literature. Alzheimer Dis Assoc Disord 1997; 11(suppl 6):135–145.
2. Alloul K, Souriol L, Kennedy W, et al. Alzheimer's disease: a review of the disease, its epidemiology and economic impact. Arch Gerontol Geriatr 1998;27:189–221.
3. Ernst RL, Hay JW. The US economic and social costs of Alzheimer's disease revisited. Am J Public Health 1994;84:1261–1264.
4. Liang K, Zeger S. Longitudinal data analysis using generalized linear models. Biometrika 1986;73:13–22.
5. Health Care Financing Review. Statistical Supplement, Table 23. Discharges, total days of care, total charges, and program payments for Medicare beneficiaries discharged from short stay hospitals, by type of entitlement: calendar years 1972–95. Washington, DC: HCFA, 1997.
6. Health Care Financing Review. Statistical Supplement, Table 26. Discharges, total days of care, and program payments for Medicare beneficiaries discharged from short-stay hospitals, by principal diagnoses within Major Diagnostic Classification (MDC): Calendar Year 1993; and Table 28. Number of discharges with a procedure, total days of care, and program payments for Medicare beneficiaries discharged from short-stay hospitals, by principal procedure within major procedure classification (MPC): calendar year 1993. Health Care Financ Rev 1995;16:202–204, 213–215.
7. Medicare Current Beneficiary Survey. Health and health care of the Medicare population (1994). http://www.hcfa.gov/mcbs/PublDT.asp; July 7, 1999.
8. Ganguli M, Seaberg E, Belle S, Fischer L, Kuller LH. Cognitive impairment and the use of health services in an elderly rural population: the MoVIES project. Monongahela Valley Independent Elders Survey. J Am Geriatr Soc 1993;41:1065–1070.
9. Weiler PG, Lubben JE, Chi I. Cognitive impairment and hospital use. Am J Public Health 1991;81:1153–1157.
10. Welch HG, Walsh JS, Larson EB. The cost of institutional care in Alzheimer's disease: nursing home and hospital use in a prospective cohort. J Am Geriatr Soc 1992;40:221–224.

AIDS- and non–AIDS-related PML association with distinct p53 polymorphism

Article abstract—A population-based analysis of progressive multifocal leukoencephalopathy (PML) showed PML frequencies of 5.1% among patients with AIDS and 0.07% among patients with hematologic malignancies, but similar clinical features of PML in both groups. Sequencing of the p53 gene, exon 4, showed heterozygosity (Arg-Pro) at codon 72 in five of six PML patients. These findings indicate that frequencies of non–AIDS- and AIDS-related PML differ markedly but p53 polymorphisms may influence the occurrence of PML in both groups. **Key words:** Progressive multifocal leukoencephalopathy—AIDS—p53 polymorphism.

NEUROLOGY 2000;54:743–746

C. Power, MD; J.G. Brown Gladden, PhD; W. Halliday, MD; M.R. Del Bigio, MD, PhD; A. Nath, MD; W. Ni, MSc; E.O. Major, PhD; J. Blanchard, MD, PhD; and M. Mowat, PhD

Progressive multifocal leukoencephalopathy (PML) is a demyelinating CNS disease caused by the papovavirus, JC virus (JCV).[1] PML has been infrequently associated with systemic immune suppression or hematologic malignancies, although[2] recently PML has become more common, affecting 5 to 7% of patients with AIDS.[1] The frequency of non–AIDS-related PML

From the Department of Clinical Neurosciences (Dr. Power and W. Ni), University of Calgary, Alberta; Departments of Pharmacology and Therapeutics (Dr. Power), Pathology (Drs. Halliday and Del Bigio), and Medical Microbiology (Dr. Blanchard), University of Manitoba, and Manitoba Institute for Cell Biology (Drs. Gladden and Mowat), Winnipeg, Canada; Department of Neurology, Microbiology and Immunology (Dr. Nath), University of Kentucky, Lexington; and Laboratory of Molecular Medicine and Neuroscience (Dr. Major), National Institute of Neurological Disorders and Stroke, Bethesda, MD.

Supported in part by the Medical Research Council (C.P. and M.M.). C.P. is a MRC Scholar and J.B.G. is a G.H. Sellers Fellow.

Received July 27, 1999. Accepted in final form October 1, 1999.

Address correspondence and reprint requests to Dr. C. Power, Department of Clinical Neurosciences, University of Calgary, Calgary, Alberta, Canada T2N 4N1.

Copyright © 2000 by the American Academy of Neurology

Table *Demographic and clinical features of patients with progressive multifocal leukoencephalopathy (PML)**

PML groups	Mean age,† y ± SE	Sex, M:F	PML risk factor‡	Biopsy/autopsy	Mean survival, mo ±SE‡
AIDS (n = 9)	35 ± 7	9:0	HIV-1	2/1	4 ± 2
Non-AIDS (n = 4)	59 ± 2	2:2	ALL (n = 1), CLL (n = 1), SLE (n = 1), NHL (n = 1)	2/1	3 ± 1

* Nineteen patients were identified by searching the databases, described in the Materials and Methods section, but six patients were excluded from the present study because they did not meet the outlined diagnostic criteria.
† Median ages were significantly different (*t* test; $p < 0.01$).
‡ Long-term survivors (n = 2) were excluded.

ALL = acute lymphocytic leukemia; CLL = chronic lymphocytic leukemia; SLE = systemic lupus erythematosis; NHL = non-Hodgkin's lymphoma.

and its clinical features compared with AIDS-related PML remain uncertain. For both AIDS- and non–AIDS-related PML, the survival prognosis is poor (3 to 6 months), although recent studies suggest that some patients may be long-term survivors of PML.[2] p53 expression is increased in PML lesions, but specific mutations in the p53 gene associated with PML have not been described.[3] p53 polymorphisms at codon 72 of exon 4 have been associated with increased frequencies of cervical carcinoma, caused by a virus related to JCV, human papilloma virus (HPV).[4] In the present study, we performed a population-based analysis of PML frequency and clinical features in patients with AIDS and non–AIDS patients and examined the relationship between p53 polymorphisms and PML occurrence.

Materials and methods. Clinical and laboratory data were obtained on all patients with PML diagnosed in the province of Manitoba, Canada, between January 1986 and December 1996 by using the ICD-9-CM code 046.3 to search for 1) all patients discharged, autopsied, or undergoing biopsies at the Health Sciences Center (HSC) and St. Boniface Hospital, the two tertiary care centers in the province; 2) all hospital discharge abstracts submitted to Manitoba Health; and 3) all patients seen in the NeuroAIDS Clinic (HSC) from 1986 to 1996. The diagnosis of PML was based on 1) clinical records (subacute, progressive, focal neurologic signs leading to death) with supportive neuroimaging (cranial MRI detection of multiple nonenhancing white matter lesions in the absence of mass effect) or 2) neuropathologic confirmation (demyelination; hyperchromatic oligodendroglial nuclei; and hypertrophied bizarre astrocytes) on autopsy or biopsy specimens, confirmed by electron microscopic or in situ hybridization detection of JC virus[5] if required to establish the diagnosis. Among patients from whom biopsy or autopsy material was available, immunocytochemistry to detect p53 (Dako, Carpenteria, CA; 1:400) was performed. To obtain p53 DNA sequence data, DNA was isolated from paraffin embedded tissue by deparaffinization with xylene, rinsing with 100% ethanol, digestion with proteinase K, followed by phenol/chloroform extraction. Exon 4 of p53 was amplified using the PCR. Primers 5′-GAGGACCTGGTCCTCTGACTG-3′ and 5′-CTCAGGGCAACTGACCGTGCA-3′ were used in 50 μL total PCR reaction volumes. PCR amplification was conducted for 30 cycles (94 °C for 1 minute; 51 °C for 1 minute; 72° C for 1 minute) producing a 335 bp product that was sequenced using an ABI 310 automated DNA sequencer.

Results. *Demographic features.* Over the 11-year period examined, 13 patients were confirmed with diagnosis of PML in Manitoba (population 1,136,400 in 1995). Nine

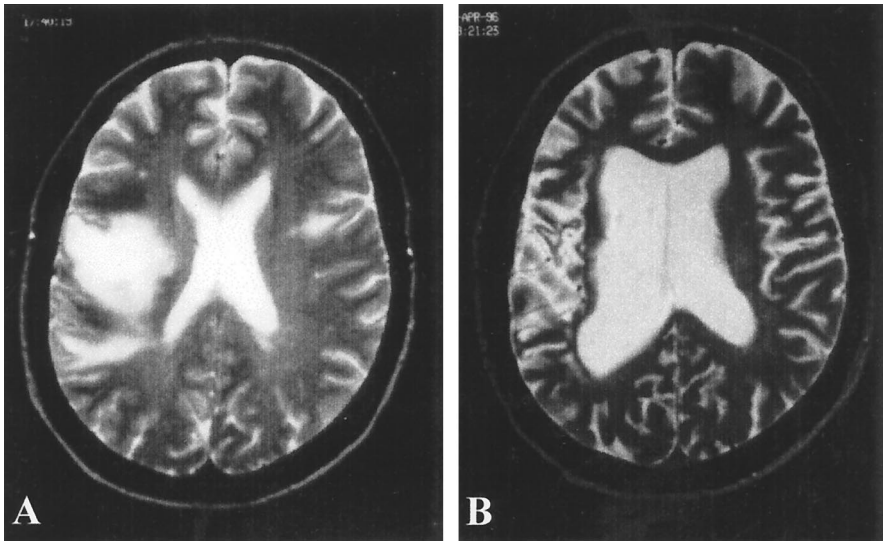

Figure 1. Sequential T2-weighted MRI scans of a non–AIDS-related PML patient with acute lymphocytic leukemia before diagnosis (A) and 200 weeks after diagnosis (B). Despite an aggressive course of cytarabine, some residual scarring in the lesion site was present at 200 weeks.

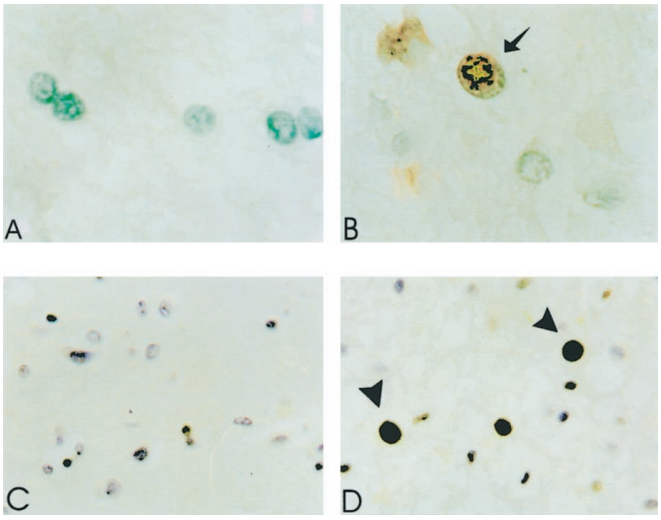

Figure 2. Representative in situ hybridization detection of JC virus (A, B) and immunocytochemical detection (C, D) of p53 in non-PML controls (A, C) and PML patients (B, D) in 10 μm brain sections. JC virus was detected in oligodendrocytes (arrow) and bizarre astrocytes in both AIDS and non–AIDS PML patients but not in controls. p53 immunoreactivity was exhibited oligodendrocytes (arrowheads) of all PML cases examined, but not in controls. H-E, original magnification × 1,000 (A, B) before 24% reduction or × 500 (C, D) before 24% reduction.

had AIDS-related PML, whereas the remaining 4 patients had coexisting immunosuppressive conditions without HIV seropositivity (table 1). All AIDS-related PML patients were male, and the risk factors for HIV infection included gay/bisexual (n = 7) and intravenous drug abuse (n = 2). The mean ages (years) at onset of PML of AIDS- (35 ± 7) and non–AIDS-related (59 ± 2) PML cases differed significantly. Biopsy and/or autopsy confirmation of PML was performed in 7 patients. The frequency of PML detection among all AIDS patients in Manitoba during this period was 5.1%, based on the number of AIDS cases in the Manitoba Health notifiable disease registry (unpublished data: Communicable Disease Control Unit, Statistical Update on HIV/AIDS, Manitoba Health). In contrast, the frequency of non–AIDS-related PML among all patients with hematologic malignancies was 0.07% over this period (unpublished data: Manitoba Cancer Treatment and Research Foundation-Annual Statistics Reports).

Clinical features. The most common presenting symptoms among both PML groups were focal weakness (n = 13), speech difficulties (n = 9), gait dysfunction (n = 8), sensory dysfunction (n = 8), and confusion (n = 4). Initial signs included focal weakness (n = 13), gait abnormalities (n = 10), cognitive impairment (n = 5), visual impairment (n = 3), and seizures (n = 1). Presenting clinical features were similar for AIDS and non-AIDS PML patients. Cranial MRI and CT scans were performed in all patients and showed hemispheric lesions in 10 patients and posterior fossa lesions in 3 patients (AIDS-related PML, n = 3), with contrast enhancement observed in 2 patients. Among patients with AIDS, the mean CD4 cell count in blood was <100 cells/mm^3 in all patients. The mean survival time for all PML patients was 52 ± 87 weeks (range 8 to 260). Two PML patients survived greater than 2 years: 1 male with AIDS who was treated with highly active antiretroviral therapy (3TC [lamivudine], saquinavir, AZT [zidovudine], cidofovir) and splenectomy[6] and survived for 130 weeks, and a non–AIDS-related patient (1 female, 52 years of age) with acute lymphocytic leukemia, treated with seven courses of cytarabine (100 mg × 5 days) over 8 months and remains alive after 5 years. Both patients displayed marked improvement in neuroimaging studies after treatment (figure 1).

Viral detection and p53 findings. Biopsy or autopsy brain tissue was available for analysis from six patients including three AIDS- and three non–AIDS-related patients with PML and two AIDS controls without PML. JC virus genome was detected in oligodendrocytes or dysmorphic astrocytes in four PML patients by in situ hybridization (figure 2A) but JC virus was identified by electron microscopy in the remaining two PML patients. JC virus was not detected in controls. Similar to other reports, all PML patient samples exhibited p53 immunoreactivity, principally localized within demyelinating lesions (see figure 2B), but it was not present in controls. Both p53 immunoreactivity and JC virus detection were associated with the extent of inflammatory cell infiltration observed near the lesion for all patients. To further examine the p53 gene, exon 4 of the p53 gene was sequenced in 6 patients (non–AIDS [n=3] and AIDS [n=3] -related PML). A polymorphism at codon 72 was observed in 5 patients (83%) who were heterozygous for arginine-proline (Arg-Pro), and one patient (AIDS) was homozygous, arginine-arginine (Arg-Arg), at the same residue.

Discussion. Previous studies have suggested that PML is a rare disease among non–HIV-infected persons,[1] usually identified in the context of systemic immune suppression or malignancy. The present study is the first epidemiologic analysis of non–AIDS-related PML, disclosing a frequency of 0.07% among all patients with hematologic malignancies in Manitoba. This study is also the first systematic comparison of AIDS and non-AIDS PML, showing that the neurologic and neuropathologic features and survival times were similar for both groups. Long-term survivors of PML were identified in each group, both of whom received aggressive treatment of their underlying illness. Recent reports from Berger et al.[2] indicate that AIDS patients with PML may exhibit long-term survival without aggressive treatment, suggesting that JCV strain differences or host resistance factors may also affect survival.

The p53 gene has been shown to modulate genotoxic stresses and expression of cellular or viral oncogenes, leading to regulation of apoptosis.[7] Altered p53 expression has been implicated in viral infections, including JC virus.[3] The current results indicate that arginine-proline heterozygosity at codon 72 of exon 4 of p53 was closely associated with PML occurrence in a subset of patients (83%). A previous report of p53 sequences from PML patients indicates that all sequences were wild type but did not specify mutation types.[3] In a recent Manitoba lung cancer study, we found the following frequencies: Pro homozygosity was 3%; Arg-Pro heterozygosity was

33%; and Arg homozygosity was 64% (unpublished data). The frequency of Arg-Pro heterozygosity in other populations was 16% and 27% in populations with lung or cervical cancers.[8,9] Hence, the present study implies that Arg-Pro heterozygosity may be abnormally high among patients with PML. The large T antigen of JC virus interacts with p53 to inhibit viral replication.[10] Thus, the finding of a polymorphism in p53 associated with PML may reflect altered large T-antigen binding and subsequent p53 function, as proposed for HPV in which the E6 protein interacts with p53, and, depending on the p53 polymorphism, modulates degradation of p53.[4] Future studies of larger numbers of PML patients and controls may permit a more definitive understanding of host factors influencing the development of PML.

References

1. Johnson RT. Viral infections of the nervous system. 2nd ed. New York: Lippincott-Raven, 1998:242.
2. Berger JR, Levy RM, Flomenhoft D, Dobbs M. Predictive factors for prolonged survival in acquired immunodeficiency syndrome: associated progressive multifocal leukoencephalopathy. Ann Neurol 1998;44:341–349.
3. Ariza A, von Uexkull-Guldeband C, Mate J, et al. Accumulation of wild-type p53 protein in progressive multifocal leukoencephalopathy: a flow cytometry and DNA sequencing study. J Neuropathol Exp Neurol 1996;55:144–149.
4. Storey A, Thomas M, Kalita A, et al. Role of p53 polymorphism in the development of human papillomavirus-associated cancer. Nature 1998;393:229–234.
5. Aksamit AJ, Sever JL, Major EO. Progressive multifocal leukoencephalopathy: JC virus detection by in situ hybridization compared with immunohistochemistry. Neurology 1986;36: 499–504.
6. Power C, Nath A, Aoki FY, Del Bigio M. Remission of progressive multifocal leukoencephalopathy following splenectomy and antiretroviral therapy in a patient with HIV infection. N Engl J Med 1997;336:661–662.
7. Teodoro JG, Branton PE. Regulation of apoptosis by viral gene products. J Virol 1997;71:1739–1746.
8. Birgander R, Sjalander A, Rannug A, et al. p53 polymorphisms and haplotypes in lung cancer. Carcinogenesis 1995; 16:2233–2236.
9. Rosenthal AN, Ryan A, Al-Jehani RM, Storey A, Harwood CA, Jacobs IJ. p53 codon 72 polymorphism and risk of cervical cancer in UK. Lancet 1998;352:871–872.
10. Staib C, Pesch J, Gerwig R, et al. p53 inhibits JC virus DNA replication in vivo and interacts with JC virus large T-antigen. Virology 1996;219:237–246.

Positive CSF HSV PCR in patients with GBM: A note of caution

Article abstract—Because two patients with temporal lobe glioblastomas had herpes simplex (HSV) DNA detected in CSF using PCR at the time of their presentation, we reviewed our laboratory's experience and performed PCR on a bank of 159 frozen CSF samples from patients with glioblastoma multiforme and other neurologic disorders. Based on the inability to detect HSV in any other tumor sample, we conclude that the positive HSV PCR in our two index patients most likely represented false-positive results. A diagnosis of HSE should not be made by PCR alone when the clinical presentation is atypical. **Key words:** Polymerase chain reaction—Herpes simplex—Glioblastoma multiforme—Cerebrospinal fluid.

NEUROLOGY 2000;54:746–749

S.S. McDermott, MD; P.F. McDermott, PhD; J. Skare, MD; M. Glantz, MD; T.W. Smith, MD; N.S. Litofsky, MD; and L.D. Recht, MD

Because numerous other diseases can mimic herpes simplex encephalitis (HSE),[1] brain biopsy was considered the best way to confirm the diagnosis until recently. Because the administration of the antiviral agent acyclovir is relatively nontoxic, physicians have been reluctant to subject their patients to the morbidity of a brain biopsy.

Recent studies have shown that amplification of HSV DNA from CSF using PCR techniques is virtually diagnostic for HSE with a sensitivity and specificity equaling or exceeding that of brain biopsy.[2,3]

Because of this test's high specificity, we were struck by the observation of positive PCR results in two adult patients with the virtually identical presentation of isolated seizure and a right temporal lesion consistent with encephalitis. Evidence of progression on imaging studies was then noted despite a full course of acyclovir treatment. On pathologic review, both patients proved to have glioblastoma multiforme (GBM). We sought to address whether this finding represented a heretofore unrecognized link between herpetic infection and glioblastoma.

Case reports. *Case 1.* A 45-year-old man presented with four generalized tonic-clonic seizures. His medical

From the Departments of Neurology (Drs. S.S. McDermott, P.F. McDermott, and Recht), Medicine (Dr. Skare), Pathology (Dr. Smith), and Surgery (Neurosurgery) (Drs. Litofsky and Recht), University of Massachusetts Medical School, Worcester, MA; and the Department of Clinical Neurosciences (Dr. Glantz), Brown University Medical School, Providence, RI.

Supported in part by NIH CA68426.

Presented in part at the 1998 meeting of the American Neurological Association.

Received June 30, 1999. Accepted in final form September 24, 1999.

Address correspondence and reprint requests to Dr. Lawrence Recht, Department of Neurology, UMASS Memorial Medical Center, 55 Lake Ave. North, Worcester, MA 01655.

Copyright © 2000 by the American Academy of Neurology

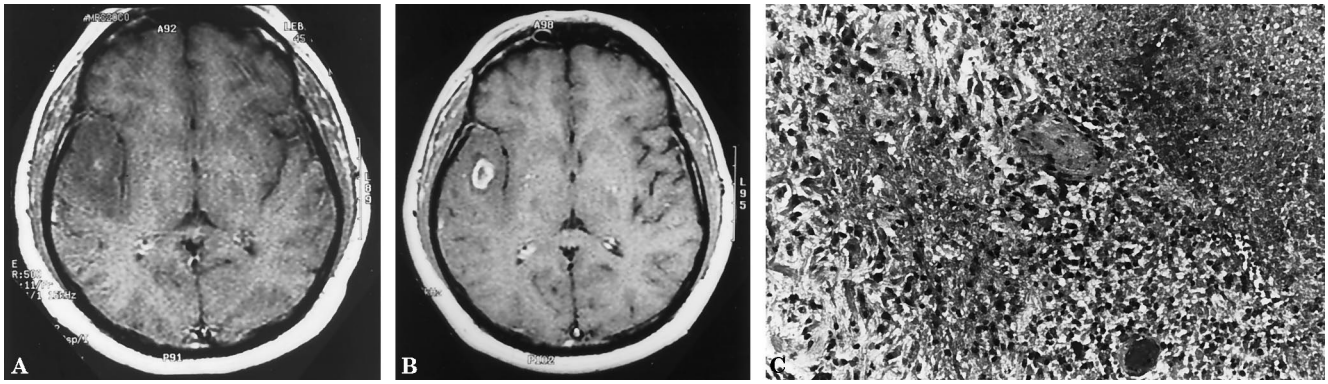

Figure. Case 1. MR scan performed at time of initial presentation (A) and 1 month later (B). At the time of presentation, a small area of enhancement was noted in a larger area of T_1-weighted hypointensity after gadolinium infusion (A). One month later, there was a marked increase in the amount of nodular enhancement on T_1-weighted images (B). Surgical excision was then performed and a glioblastoma with features of oligodendroglioma was identified (C). Immunohistochemistry for HSV antigens on the resected sample was negative.

history was significant for a remote history of optic neuropathy. He had a headache and neck pain. He was somewhat lethargic. CSF examination revealed one leukocyte and five erythrocytes/mm^3; CSF protein was 51 mg/dL and the glucose was 95 mg/dL. One atypical oligoclonal band in his CSF was noted. A PCR analysis for HSV was positive. MR imaging (figure, A) showed a 4.5-cm, nonenhancing right temporal lesion with minimal edema and a small area of hemorrhage.

For 21 days, the patient was treated with IV acyclovir, 30 mg/kg per day. A repeat MRI (figure, B) showed the presence of a new contrast-enhancing component of the lesion. Surgical resection was therefore performed. Pathologic examination showed a GBM with some oligodendroglial features (figure, C). Immunohistochemical assessment for HSV showed no evidence of viral antigen in the tumor tissue.

The patient survived 2 years. Neither another CSF analysis nor postmortem examination was performed.

Case 2. A 63-year-old man with no significant medical history had a headache and then was found unresponsive a short time later. He then had a generalized tonic-clonic seizure. He was afebrile with normal vital signs. Initially, he was disoriented but returned to his baseline within 15 minutes. Unenhanced CT of his brain was normal. A contrast-enhanced MRI showed a hypointense area in the right temporal lobe; three small enhancing nodules were noted within the area. CSF analysis revealed one erythrocyte and two leukocytes/mm^3; protein was 45 mg/dL and glucose was 66 mg/dL with a serum glucose of 101 mg/dL. Gram stain of the CSF was normal. PCR for HSV was positive.

For 21 days, the patient was treated with IV acyclovir, 30 mg/kg per day. A repeat MRI of his brain at the end of therapy showed increased size of the enhancing nodules. Surgical resection of a pathologically confirmed GBM was performed. Immunohistochemical stains of tumor tissue for HSV antigens were negative.

The patient died 10 months later. Neither a postmortem examination nor another CSF analysis was obtained.

Materials and methods. The results of all CSF PCR analyses performed at the UMMHC laboratories between January 1, 1997, and December 30, 1997, were reviewed along with charts from patients with positive results.

Because previous studies by other workers suggest that freezing does not destroy target DNA,[4] we also analyzed 159 frozen CSF specimens obtained from patients older than 18 years with varied neurologic diagnoses for the presence of HSV DNA using PCR. PCR amplification was performed using oligonucleotide primers homologous to a 476-nucleotide region of the DNA polymerase gene of HSV1 and HSV2 as reported previously.[5] The primer sequences were: 5′-CAGTACGGCCCCGAGTTCGTGA-3′ and 5′-GTAGATGGTGCGGGTGATGTT-3′. DNA was extracted from 10 and 30 μL of CSF and then amplified. One plaque-forming unit (PFU) of HSV DNA was added to additional reactions to determine whether specimens had inhibitors of the amplification process.

Results. To address the possibility that the positive PCR results in our patients represented a false-positive result based on laboratory methodology, we analyzed our records for positive results obtained during calendar year 1997. Of 106 CSF samples tested, 6 (5.7%) were positive (including those of the 2 patients in this report). Of the other four positive PCR samples, one was highly likely to be a false-positive. This patient was a 57-year-old man who sustained a closed-head injury after which status epilepticus developed. A CT scan was normal, as was initial CSF analysis, other than the PCR.

To ascertain further the relationship between positive PCR and the development of brain tumor, we extracted DNA from the paraffin block containing the tumor from Case 1. No HSV DNA could be detected. In addition, we also analyzed a bank of frozen CSF samples for the presence of HSV DNA using the same technique as that used by the clinical laboratory. This cohort included: 1) patients with a known glial tumor (29%); 2) patients with another type of brain tumor (20%); 3) patients with systemic cancer but no CNS involvement (33%); and 4) patients with no known cancer who underwent lumbar puncture for evaluation of other neurologic conditions. In all cases, PCR analysis was negative for the presence of HSV.

Discussion. PCR is a rapid, highly sensitive, noninvasive method for the diagnosis of CNS herpetic infection that can identify viral invasion of the CNS at an early stage.[6] The use of PCR in combination

with the detection of a specific intrathecal antibody response to HSV currently represents the most reliable strategy for diagnosing and monitoring the treatment of adult patients with HSE, having been used as a diagnostic criterion in a recent article dealing with long-term outcomes from HSE.

It has long been recognized that mild or atypical presentations of HSE occur. Because perhaps up to 20% of cases may be atypical, some have recommended that PCR should be performed in all patients with febrile encephalopathy, even in the absence of focal features, initial CSF pleocytosis, or abnormal CT scans.

In the context of its high specificity and sensitivity, the presence of HSV by PCR analysis in the two presented cases raises the question of whether a heretofore undetected association exists between HSV infection and the development of primary brain tumor. Other possibilities need to be considered, however, including whether these results resulted from unintentional contamination in the laboratory with HSV, whether the positive result represents a coincident reactivation of a latent herpetic condition, or whether it reflects latent residence in CNS tissues.[7]

Although the presence of a positive PCR in a patient with a nondominant lobe tumor could suggest an etiologic link between herpetic infection and the development of glioma, several points mitigate against this association. First, the tumor itself was negative for HSV by both immunohistochemistry and PCR. Second, unlike the relationship between EBV and CNS lymphoma and leiomyosarcoma, there is little evidence to suggest an etiologic role for herpesvirus in the development of glioma. In a recent review of possible etiologic factors of brain tumors, for example, HSV is not even considered.[8] Furthermore, we could not document another positive HSV PCR result in any other brain tumor patient whose CSF was examined.

We also do not believe that the positive results reflected either reactivation or new infection that occurred in the setting of the immunosuppression, which has been noted in patients with brain tumor.[9] Although the first patient did have a remote history of optic neuropathy, there was no ophthalmologic evidence of ocular pathology at the time of tumor presentation, and neither the patient's CSF profile nor presentation was suggestive of an active herpetic infection. Second, the lack of another positive PCR result among our banked CSF specimens suggests that such a finding is not frequent. Finally, when HSE does develop in patients with primary brain tumors, florid syndromes occur and the reported patients have had pathologic verification of virus in the tumor bed.[10] Nevertheless, reactivation remains a possible explanation, and because the primers used cannot distinguish between HSV-1 and HSV-2, one cannot even ensure that this positive result did not represent the presence of HSV-2.

Despite the striking similarity of these two cases, the possibility that these results reflected false-positives must also be considered. The techniques used in our laboratory are very similar to those reported in the literature,[2,5] so it is unlikely that these positives reflected a technical artifact. Even if we assume that the results of the 2 patients with GBM were false-positive and that there were no false-negative assay results in the 106 evaluable cases from our laboratory in the year surveyed, the overall sensitivity and specificity of this test would still be 100% and 97%, respectively. If the 159 patients with banked CSF are added, the specificity increases to 99%. Given these figures, however, observing three false-positives is certainly possible, even if two of these results occurred in patients with similar presentations and imaging studies. Given that none of the 130 patients with CNS or systemic cancer (many of whom were more immunocompromised than the 2 index patients) had positive results, we believe this is a more likely explanation than latent reactivation, although further studies will be needed to definitively distinguish between the 2 alternatives.

Whatever the reason, however, the most important conclusion of this study is that a note of caution must be made about overinterpreting positive PCR results for HSV. Although neither patients' eventual care suffered as the result of receiving 3 weeks of acyclovir treatment (although this agent clearly had no effect on tumor progression), we would recommend that if the remaining data do not support the diagnosis, especially when the CSF is otherwise normal, then physicians should not rely exclusively on HSV PCR to guide their management. We therefore recommend definitive tissue diagnosis via biopsy as the preferred management strategy to minimize the delay in initiating appropriate treatments.

Acknowledgment

The authors thank Rebecca Salmonsen, MS, for expert technical assistance and Dr. George Perides, New England Medical Center, for providing CSF samples.

References

1. Whitley RJ, Cobbs CG, Alford CA, et al. Diseases that mimic herpes simplex encephalitis. Diagnosis, presentation, and outcome. JAMA 1989;262:234–239.
2. Aurelius E, Johansson B, Skoldenberg B, Staland A, Forsgren M. Rapid diagnosis of herpes simplex encephalitis by nested polymerase chain reaction assay of cerebrospinal fluid. Lancet 1991;337:189–192.
3. Lakeman FD, Whitley RJ, NIAID-Collaborative Antiviral Study Group. Diagnosis of herpes simplex encephalitis: application of polymerase chain reaction to cerebrospinal fluid from brain-biopsied patients and correlation with disease. J Infectious Dis 1995;171:857–863.
4. Villanueva AV, Podzorski RP, Reyes MP. Effects of various handling and storage conditions on stability of Treponema pallidum DNA in cerebrospinal fluid. J Clinical Microbiology 1998;36:2117–2119.
5. Rogers BB, Josephson SL, Mak SK. Detection of herpes simplex virus using the polymerase chain reaction followed by endonuclease cleavage. Am J Pathology 1991;139:1–6.
6. Aslanzadeh J, Osmon DR, Wilhelm MP, Espy MJ, Smith TF. A prospective study of the polymerase chain reaction for detec-

tion of herpes simplex virus in cerebrospinal fluid submitted to the Clinical Virology Laboratory. Mol Cell Probes 1992;6: 367–373.
7. Baringer JR, Pisani P. Herpes simplex virus genomes in human nervous system tissue analyzed by polymerase chain reaction. Ann Neurology 1994;36:823–829.
8. Inskip PD, Linet MS, Heineman EF. Etiology of brain tumors in adults. Epidemiol Rev 1995;17:382–414.
9. Weller M, Fontana A. The failure of current immunotherapy for malignant glioma. Tumor-derived TGF-b, T-cell apoptosis, and the immune privilege of the brain. Brain Res Rev 1995;21: 128–151.
10. Schiff D, Rosenblum MK. Herpes simplex encephalitis (HSE) and the immunocompromised: a clinical and autopsy study of HSE in the settings of cancer and human immunodeficiency virus-type 1 infection. Hum Pathol 1998;29:215–222.

Natural history of aortic arch atherosclerotic plaque

Article abstract—To define the natural history of aortic arch plaque, we used B-mode ultrasonography to perform sequential study of the aortic arch. Eighty-nine patients were studied for up to 18 months. There was no change in 67% of total plaques; 77% of simple plaque (<4 mm) and 48% of complex plaque (≥4 mm) did not progress. Atherosclerosis of the aortic arch can be sequentially studied with B-mode ultrasonography, and most of these lesions remain unchanged after up to 18 months of observation. **Key words:** Aortic arch—Atherosclerosis—Cerebrovascular disease—B-mode ultrasonography.

NEUROLOGY 2000;54:749–751

Anthony Geraci, MD; and Jesse Weinberger, MD

Atherosclerosis of the aortic arch was first implicated as a source of embolic stroke >40 years ago.[1] The available technology at that time and during the ensuing 2 decades made in vivo assessment of the wall of the aortic arch untenable. The advent of transesophageal echocardiography (TEE) renewed interest in the aortic arch and encouraged the development of improved techniques for studying atherosclerotic disease. Several investigators have reported on atherosclerosis of the aortic arch as a potential source of systemic emboli and an independent risk factor for ischemic stroke.[2-6]

Current research implicates aortic arch plaque as an etiologic factor in stroke and also defines plaque characteristics associated with a higher stroke risk such as wall thickness and protruding or mobile elements. However, studies to date have been cross-sectional and do not include follow-up data, probably because of the inherent difficulties of performing serial TEE. Emerging studies seek to assess therapeutic effectiveness in patients with aortic arch plaque[7] and will become increasingly important to understand the natural history of these lesions and how that might be altered by prospective pharmacologic interventions. The current study seeks to answer this question by using B-mode ultrasonography for sequential study of the aortic arch in patients with known or suspected cerebrovascular disease.

From the Department of Neurology, The Mount Sinai School of Medicine, New York, NY.

Received June 2, 1999. Accepted in final form September 22, 1999.

Address correspondence and reprint requests to Dr. Jesse Weinberger, Department of Neurology, Box 1052, The Mount Sinai School of Medicine, 1 Gustave Levy Place, New York, NY 10029.

Methods. Serial evaluations of the aortic arch were performed on patients using B-mode ultrasonography over the course of up to 18 months. Patients were referred for clinical neurovascular evaluation including carotid Doppler and transcranial Doppler examination. Referrals were nonconsecutive and were made from April 1997 to October 1998. Forty percent of referrals were made because of symptoms of transient ischemic attack or amaurosis fugax, 18% were made because of asymptomatic carotid bruit, and 42% were made because of other nonspecific symptoms such as dizziness. Follow-up studies were done at random intervals based on when patients were referred back for evaluation. All patients who had a baseline evaluation and returned for follow-up were included in the analysis.

B-mode ultrasonography of the aortic arch was performed with an Acuson XP 128 colorflow duplex Doppler instrument (Acuson, Mountain View, CA) using an L7-phased array linear probe at 7.5 MHz. A lateral supraclavicular approach was used to visualize the distal ascending aorta, aortic arch, and proximal descending aorta, as described previously.[8] Aortic arch plaques were characterized as simple if the aortic wall thickness was <4 mm and complex if it was ≥4 mm. A change in plaque size was defined as a difference of ≥0.5 mm. All evaluations were performed by the same investigator (J.W.) who had knowledge of previous results when performing follow-up studies. Although it is possible that new plaques may have formed during follow-up and prior plaques may have disappeared, a false-positive result was defined as a plaque seen on initial study that was not present on follow-up and a false-negative study was defined as a plaque seen on follow-up that was not seen on the initial study. Intraobserver reliability was assessed by taking the ratio of the sum of false-positive and false-negative results to the total number of observations. Because this was an observational study without an experimental variable, statistical comparisons were not made.

Copyright © 2000 by the American Academy of Neurology

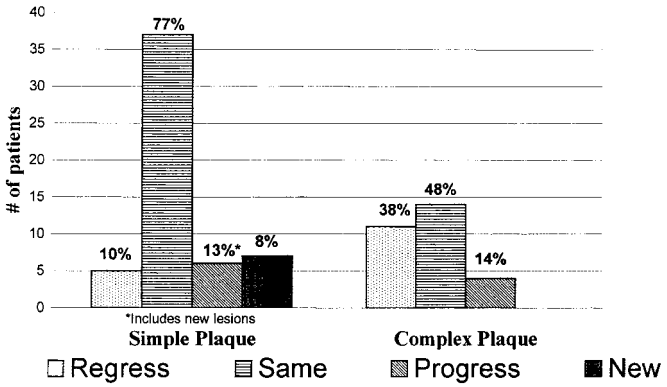

Figure. Change of aortic arch plaque size in simple and complex plaque groups.

Results. Eighty-nine patients were studied with a total of 100 follow-up evaluations. Patient ages ranged from 54 to 90 years with a mean age of 74 years. Follow-up intervals ranged from 3 to 18 months with a mean of 7.7 months. Twenty-one percent of follow-up studies were completed at 3 months, 53% between 6 and 9 months, and the remaining 26% of patients were restudied at 1 year to 18 months. At baseline, 46 patients were identified with simple plaque, 27 with complex plaque, and 16 patients had a normal aortic arch. There was no change seen in the thickness of the aortic wall in 67% of the total follow-up studies. There was no change in 77% of patients with simple plaque and 48% with complex plaques (figure). There was regression in 38% of patients with complex plaque and progression in only 14%. Only 13% of patients in the simple plaque group had progression of aortic arch plaque. Seven patients (8%) who were normal at baseline had a new lesion identified at follow-up. A second new lesion on the roof of the aorta was seen in two patients. Two patients regressed from complex to simple plaque; however, none of the patients progressed from simple to complex plaque. The overall intraobserver reliability was 90%.

Discussion. Most patients in our observational cohort had atherosclerosis of the aortic arch. It is possible to perform sequential evaluation of the aortic arch using B-mode ultrasonography. We previously have shown that this method is both sensitive (94%) and specific (81%) for the detection of aortic arch plaque when compared with TEE.[9] Twenty consecutive stroke patients were evaluated by both methods, and B-mode ultrasonography correctly identified 13 plaques in the proximal and distal aortic arch that were visualized with TEE.[8]

Only 13% of our patients with simple plaque and 14% with complex plaque had significant progression of aortic wall thickness. However, seven patients with a normal arch at baseline had plaque develop during the follow-up period. These were all simple plaques; no new lesions were seen in the complex plaque group, probably because of the short observation period. It is possible that new plaques may have progressed to >4 mm and therefore have been categorized as complex if the observation period had been longer. Conversely, new lesions may have represented false-negatives at baseline. Although previous data comparing TEE to ultrasonography show a sensitivity approximating our intraobserver reliability in this study,[9] it is possible that knowledge of previous results may have introduced bias. False-positive and false-negative values relating to measurement of plaque size and change in plaque status are difficult to assess; however, we chose the traditional lower limit of resolution (0.5 mm) for carotid artery sonography as our definition of change in plaque size. This should mitigate against significant error when aortic arch ultrasonography is performed by an experienced sonographer.

Early reports of an association between stroke and aortic arch plaque seen with TEE[2] were of mobile and protruding elements into the lumen of the aortic arch. Subsequent studies showed that aortic arch plaques, particularly those >4 mm, are associated with an increased relative risk for ischemic stroke.[3-6] Although it seems clear that patients with complex aortic plaque and those with protruding or mobile plaque are at increased risk of experiencing stroke, our data begin to shed light on the natural history of these lesions. It may be possible to further define the plaque characteristics that are most associated with stroke. We recently reported on the association of ischemic symptoms and heterogeneous complex plaque.[9] A recent report similarly found that although there was a significant association between plaque thickness >4 mm and stroke, hypoechoic and ulcerated aortic arch plaques had a significantly higher correlation with ischemic stroke than homogeneous dense plaques.[10]

Our results suggest that there may be a subset of patients with an aggressive form of atherosclerosis. Taken together with the emerging data on the association of plaque morphology and increased stroke risk, this may allow for the identification of patients most at risk of having ischemic stroke. A recent study suggests the benefits of anticoagulation in patients with embolic stroke and mobile aortic plaque.[7] Future therapeutic trials may benefit from an ability to identify a group of patients with aortic arch atherosclerosis who are at higher risk of vascular events and whose variables might predict regression or progression of plaque size, such as cholesterol levels and the use of cholesterol-lowering agents.

References

1. Winter WJ Jr. Atheromatous emboli: a cause of cerebral infarction. Arch Pathol Lab Med 1957;64:137–142.
2. Tunick PA, Kronzon I. Protruding atherosclerotic plaque in the aortic arch of patients with systemic embolization: a new finding seen by transesophageal echocardiography. Am Heart J 1990;120:658–660.
3. Amarenco P, Cohen A, Tzourio C, et al. Atherosclerotic disease of the aortic arch and the risk of ischemic stroke. N Engl J Med 1994;331:1474–1479.
4. Jones EF, Kalman JM, Calafiore P, Tonkin AM, Donnan GA. Proximal aortic atheroma: an independent risk factor for cerebral ischemia. Stroke 1995;26:218–224.

5. The French Study of Aortic Plaques in Stroke Group. Atherosclerotic disease of the aortic arch as a risk factor for recurrent ischemic stroke. N Engl J Med 1996;334:1216–1221.
6. Mitusch R, Doherty C, Wucherpfenning H, et al. Vascular events during follow-up in patients with aortic arch atherosclerosis. Stroke 1997;28:36–39.
7. Dressler FA, Craig WR, Castello R, Labovitz AJ. Mobile aortic atheroma and systemic emboli: efficacy of anticoagulation and influence of plaque morphology on recurrent stroke. J Am Coll Cardiol 1998;31:134–138.
8. Weinberger J, Azhar S, Danisi F, Hayes R, Goldman M. A new noninvasive technique for imaging atherosclerotic plaque in the aortic arch of stroke patients by transcutaneous real-time B-mode ultrasonography. Stroke 1998;29:673–676.
9. Weinberger J, Papamitsakis N, Newfield A, Godbold J, Goldman M. Plaque morphology correlates with cerebrovascular symptoms in patients with complex aortic arch plaque. Arch Neurol 2000 (in press).
10. Cohen A, Tzourio C, Bertrand B, Chauvel C, Bousser M-G, Amarenco P. Aortic plaque morphology and vascular events: a follow-up study in patients with ischemic stroke. Circulation 1997;96:3838–3841.

Cerebral deep venous thrombosis presenting as acute micrographia and hypophonia

Article abstract—Deep cerebral venous thrombosis is often a devastating condition associated with hemorrhagic infarction. We describe a patient who presented with acute micrographia and hypophonia as the sole manifestations of extensive deep venous sinus thrombosis. **Key words:** Micrographia—Hypophonia—Cerebral venous thrombosis—Basal ganglia—Parkinsonism—Magnetic resonance venography—Heparin—Cerebral infarction—Cerebral hemorrhage.

NEUROLOGY 2000;54:751–753

B.J. Murray, MD; R. Llinas, MD; L.R. Caplan, MD; T. Scammell, MD; and A. Pascual-Leone, MD, PhD

Cerebral venous thrombosis is usually a severe illness with seizures and focal neurologic deficits. We present a patient with the acute onset of micrographia and hypophonia, an unusual presentation of thrombosis of the deep cerebral venous system.

Case report. A 62-year-old woman developed small handwriting and a soft voice in the setting of a new, dull vertex headache. She was brought to the hospital after an episode of decreased responsiveness associated with a low-frequency tremor of the right arm that resolved spontaneously. She had no significant prior medical history and was taking estrogen and progesterone hormone replacements. She occasionally used a nonsteroidal anti-inflammatory medication for rare muscle contraction-type headaches. A few days before presentation, she resumed taking this medication for her new head discomfort. A brain CT 6 months before presentation for evaluation of the headaches had shown no abnormalities.

On examination, she was afebrile and had a blood pressure of 108/53. Her general examination was normal, and she was well hydrated. On mental status examination, her digit span was normal, and her speech was fluent without paraphasic errors. However, she was hypophonic and unable to yell. Her writing was smaller than normal (figure 1). When asked to copy items, she drew them significantly smaller than the model (see figure 1). On attempting to copy a spiral, she was unable to "swing out" and became stimulus bound, despite continued reminders to get "bigger" (see figure 1). Her affect was flat as confirmed by direct questioning about her mood. She was appropriately concerned about her situation when she was told that she had a stroke. She was bradyphrenic in her conversation. The patient's cranial nerves were normal. Her motor examination showed no pronator drift, but slight right upper motor neuron weakness (5-/5 strength in deltoid, triceps, finger extensors, and hamstrings). There was no cogwheel rigidity or tremor. The patient was slightly bradykinetic in facial movements, limb movements, and gait. She reported some transient slight tingling on her right face, arm, and leg, but she had normal sensation to primary modalities as well as stereognosis and graphesthesia. Her coordination was normal. Gait was notable for reduced arm swing and small steps. Reflexes were symmetrically brisk and toes were downgoing.

A brain CT was normal except for slightly increased density at the midline edge of the upper midbrain tegmentum, which may have reflected thrombus in the vein of Galen. There were multiple abnormalities on a diffusion-weighted MRI scan including increased signal in bilateral thalami (left more than right), bilateral putamenae, and caudate nuclei (more confluent on the right), as well as areas suggestive of punctate hemorrhage in the right caudate nucleus and left thalamus on the susceptibility-weighted images (figure 2). Head magnetic resonance venogram (MRV) (see figure 2C) showed multiple venous blockages, including absent flow in the internal cerebral vein, vein of Galen, straight sinus, left transverse sinus, left sigmoid sinus, and left internal jugular vein. The left subclavian vein and superior vena cava were patent on chest MRV.

Routine blood chemistry and hematology were normal.

From the Department of Neurology, Beth Israel Deaconess Medical Center, Harvard Medical School, Boston, MA.

Received August 4, 1999. Accepted in final form September 22, 1999.

Address correspondence and reprint requests to Dr. Alvaro Pascual-Leone, Department of Neurology, Beth Israel Deaconess Medical Center, Kirstein Hall KS 452, 330 Brookline Avenue, Boston, MA 02215; e-mail: apleone@caregroup.harvard.edu

Copyright © 2000 by the American Academy of Neurology

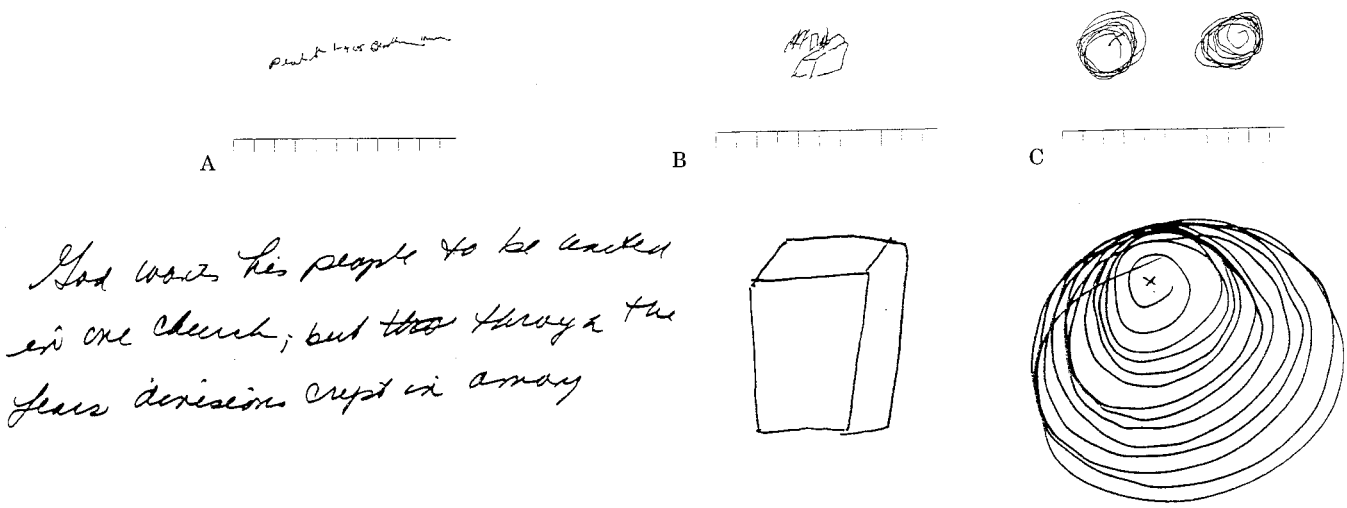

Figure 1. Items above the scale were drawn at presentation, and those below the scale were drawn 1 month later. Two tick marks represent 1 cm. (A) Writing samples. (B) Copy of a cube demonstrating initial marked reduction in size. (C) Copy of a spiral figure.

An extensive workup for malignancy was unremarkable. Her thyroid-stimulating hormone and erythrocyte sedimentation rate were normal. No clotting abnormalities were identified (i.e., normal protein C, S, factor V Leiden, homocysteine). The patient's antithrombin 3 was slightly lower than normal. The patient's anticardiolipin immunoglobulin G was elevated, but antinuclear antibody was negative, as was the lupus anticoagulant.

The patient's hormonal replacement was discontinued, and she was started on phenytoin for seizure prophylaxis and heparin, which was later converted to warfarin, to inhibit clot propagation. The MRV was repeated 3 weeks later, and flow in the internal cerebral vein and vein of Galen had improved (see figure 2F). Furthermore, not all of the areas that had abnormal diffusion signal had evolved into infarcts. There was residual T2 hyperintensity in the right basal ganglia and centrum semiovale on the right and on the left thalamus (see figure 2D). The patient's handwriting had returned to its normal size, and she was able to copy items closer to their original dimensions (see figure 1). Her attempts to draw a spiral were also clearly improved (see figure 1).

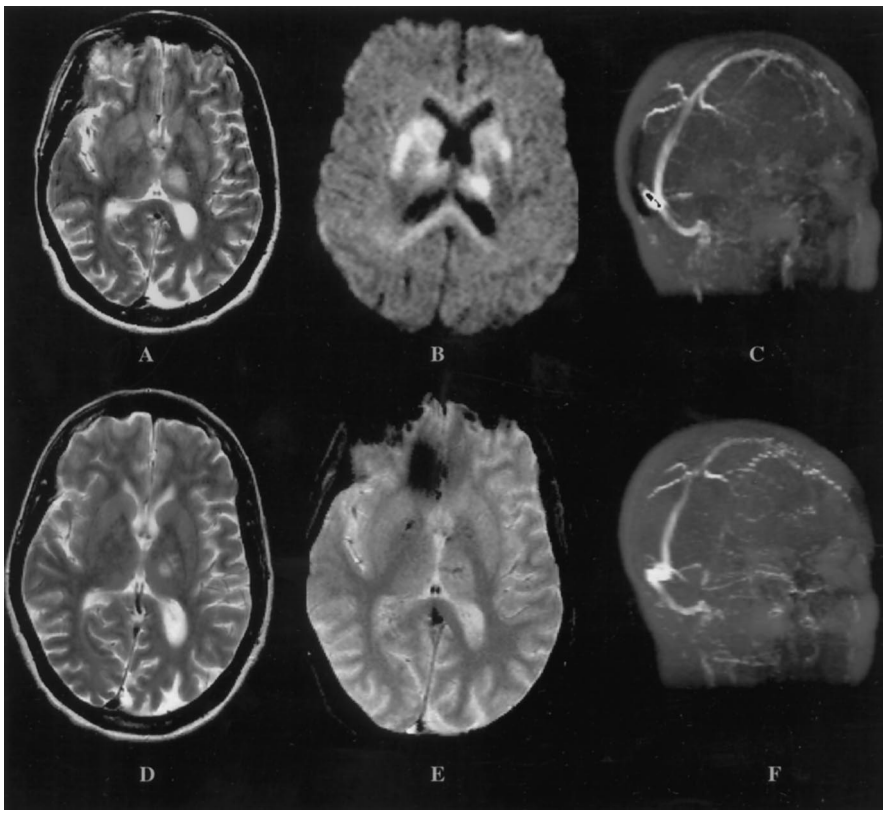

Figure 2. (A) MRI at presentation showing multiple T2 abnormalities. (B) Diffusion-weighted sequence demonstrating marked signal changes in deep structures. (C) Magnetic resonance venography (MRV) showing absent flow in the internal cerebral venous system. (D) A T2-weighted MRI 1 month later showing a few areas of infarction. (E) Susceptibility-weighted sequences demonstrating multiple areas of punctate hemorrhage. (F) MRV 1 month later demonstrating improved flow in the internal cerebral venous system.

Discussion. Our patient shows that micrographia and hypophonia can occur acutely and may suggest cerebrovascular disease. Often these findings will only be found with careful observation because they may be dwarfed by more dramatic findings. However, occasionally, a patient may spontaneously report only small handwriting and "soft speech."

Micrographia is believed to be a consequence of inappropriately "weak" movement commands in the execution of an overlearned, automatic action. It is interesting that in this patient external auditory cues (instructing the patient to draw a bigger spiral loop) were not helpful in increasing the size of the handwriting, although this did seem to assist in follow-up. Oliveira et al. reported that when patients with PD were given auditory reminders ("write big"), performance improved.[1] These authors hypothesize that micrographia is the consequence of the supplementary motor area dysfunction found in PD ("open loop" dysfunction), which can be overcome by making the task less automatic. They also reported that visual cues were helpful in activating the "closed loop" of the lateral premotor cortex (by decreasing task automaticity). Our patient's performance did not improve when provided with the direct cue of her last drawn item on a serial copying task. However, this difference could be related to differences in the underlying pathology (vascular in our patient versus an underlying degenerative process).

Micrographia and hypophonia are common symptoms of parkinsonian patients presenting to movement disorders or behavioral neurology clinics. Although common, the exact frequency of these phenomena are unknown.[2] In a retrospective chart review one series reported that 24.6% of patients with vascular parkinsonism noted the onset of their symptoms with stroke.[3] Micrographia and hypophonia may be present in a subset of these patients. It has been reported previously that the dysarthria–clumsy hand syndrome can occur with micrographia.[4] Other reported causes of this syndrome include lenticular hematoma,[5] thalamomesencephalic infarction,[6] thalamocapsular tumor,[7] and MS.[8] Our study demonstrates that micrographia and hypophonia might be presenting complaints and practically the sole finding of extensive cerebral vein thrombosis.

Deep venous systems receive inflow from both thalami and basal ganglia. Infarctions have been noted to preferentially occur in these regions with venous thrombosis.[9]

The clinical course of this patient demonstrates a successful outcome of anticoagulation for cerebral venous thrombosis, despite punctate hemorrhagic lesions. This supports the safety findings of a recent study with low–molecular-weight heparin.[10]

It is surprising that our patient had so few other findings on her neurologic examination given the severity of lesions suggested by the neuroimaging. The lack of progression of areas of restricted diffusion to infarction indicates that the initial abnormalities were most likely caused by edema and not brain ischemia. MRV is now able to detect dural sinus and cerebral vein occlusions even in patients with relatively minor clinical findings.

References

1. Oliveira RM, Gurd JM, Nixon P, Marshall JC, Passingham RE. Micrographia in Parkinson's disease: the effect of providing external cues. J Neurol Neurosurg Psychiatry 1997;63:429–433.
2. McLennan JE, Nakano K, Tyler HR, Schwab RS. Micrographia in Parkinson's disease. J Neurol Sci 1972;15:141–152.
3. Winikates J, Jankovic J. Clinical correlates of vascular parkinsonism. Arch Neurol 1999;56:98–102.
4. Noda S, Itoh H, Goda S. Micrographia due to focal cerebral lesions as seen in the dysarthria-clumsy hand syndrome. Neurology 1994;44:150–151.
5. Martinez-Vila E, Artieda J, Obeso JA. Micrographia secondary to lenticular haematoma. J Neurol Neurosurg Psychiatry 1988;51:1353. Letter.
6. Kim JS. Micrographia after thalamo-mesencephalic infarction. Neurology 1999;52:1921–1922. Letter.
7. Lewitt PA. Micrographia as a focal sign of neurological disease. J Neurol Neurosurg Psychiatry 1983;46:1152–1153. Letter.
8. Scolding NJ, Lees AJ. Micrographia associated with a parietal lobe lesion in multiple sclerosis. J Neurol Neurosurg Psychiatry 1994;57:739–741.
9. Caplan LR. Venous and dural sinus thrombosis. In: Posterior circulation disease: clinical findings, diagnosis, and management. Cambridge, MA: Blackwell Science, 1996:569–592.
10. De Bruijn SFTM, Stam J. Randomized, placebo-controlled trial of anticoagulant treatment with low-molecular-weight heparin for cerebral sinus thrombosis. Stroke 1999;30:484–488.

Acute hydrocephalus in nonketotic hyperglycinemia

Article abstract—We present four patients with typical neonatal onset nonketotic hyperglycinemia (NKH) who developed hydrocephalus requiring shunting in early infancy. Brain imaging revealed acute hydrocephalus, a megacisterna magna or posterior fossa cyst, pronounced atrophy of the white matter, and an extremely thin corpus callosum in all. The three older patients had profound developmental disabilities. This suggests that the development of hydrocephalus in NKH is an additional poor prognostic sign. **Key words:** Hydrocephalus—Nonketotic hyperglycinemia—Posterior fossa cyst—Developmental outcome.

NEUROLOGY 2000;54:754–756

J.L.K. Van Hove, MD, PhD; P.S. Kishnani, MD; P. Demaerel, MD; S.G. Kahler, MD; C. Miller, MD; J. Jaeken, MD, PhD; and S.L. Rutledge, MD

In nonketotic hyperglycinemia (NKH), deficient glycine cleavage enzyme activity produces increased glycine levels in blood and CSF, with an increased CSF to plasma glycine ratio. Infants present in the first days of life with lethargy progressing to coma, pronounced hypotonia, myoclonic seizures, and apnea. The EEG shows a burst suppression pattern. Spontaneous breathing resumes after 1 to 2 weeks. Psychomotor development is delayed, and axial hypotonia, peripheral spasticity, few spontaneous movements, poor head control, and severe seizures are common. Variant late-onset forms and transient forms have been reported.

Even in patients presenting as a neonate, developmental outcome is variable; some have moderate mental retardation and achieve independent walking, while others do not make any developmental progress. Recent studies have suggested that factors other than glycine kinetics may be important for these differences in developmental outcome, including prenatal malformations.[1,2] Reported malformations include a hypoplastic or absent corpus callosum, delayed to absent myelination,[3] gyral malformations, and cerebellar hypoplasia.[4] In this study, we describe four patients with neonatal onset NKH who developed acute hydrocephalus and a posterior fossa cyst.

Case reports. *Case 1.* In the first 3 days of life, this baby girl became hypotonic and lethargic, had clonic movements, and was intubated for apnea. Electroencephalogram showed a burst suppression pattern. The plasma glycine level was 830 μM, the CSF glycine level was 218 μM, with a CSF to plasma glycine ratio of 0.26. Urine organic acids were normal. A diagnosis of NKH was made, and she was treated with 500 mg/kg of sodium benzoate per day, 7.5 mg/kg of dextromethorphan per day, ranitidine, phenobarbital, and D-serine. A CT scan on day three of life showed mild dilatation of the lateral ventricles posteriorly greater than anteriorly, as would be seen in partial absence of the corpus callosum (figure, A). The ventricular dilatation was slightly increased at the end of the first week. There was no evidence of brain atrophy. Infantile spasms appeared at age 3½ months and were treated with vigabatrin. At age 4½ months, an acute increase in head circumference to above the 95th percentile was associated with vomiting, a bulging fontanel, and increased flexor spasms. Computed tomography scan showed pronounced enlargement of all ventricles with effacement of sulci, and decreased attenuation around the frontal horns suggestive of transependymal egress of fluid (figure, B). Dilatation of the optochiasmatic cistern suggested that hydrocephalus had been present for some time before the scan. A ventriculoperitoneal shunt was placed, and MRI showed a decreased ventricular size (figure, C). On sagittal images (figure, D), the corpus callosum was markedly thinned. There was a posterior fossa cyst that caused anterior and superior displacement of the cerebellar vermis. This was not noticeable on the images in the first week of life. There was no evidence of gyral malformations. Myelination was absent in the internal capsule and in the dorsal brainstem. Follow-up MRI 10 months later showed persistent ventriculomegaly. At age 1 year and 5 months, the patient had severe axial hypotonia, hyperreflexia, and dystonic posturing. She had no grasp reflex. She reacted to sound and touch, but not to visual stimuli. Gastrostomy tube feeding was required. Her head circumference had decreased to the 95th percentile. Medications included sodium benzoate, dextromethorphan, and vigabatrin.

Case 2. Details of this patient's history have been previously reported.[5] On the second day of life, he became hypotonic with poor sucking and with clonic jerks. He was ventilated for apnea from days 5 to 22 of life. His plasma glycine was 795 μM, and CSF glycine was 167 μM, rendering a CSF to plasma glycine ratio of 0.21. Urine organic acids were normal. The CT scan at 8 days of life showed normal sized ventricles, absence of the corpus callosum, and a small to moderate posterior fossa cyst. At diagnosis on day 36, he was hypotonic, hyperreflexic, and had frequent myoclonic seizures. After treatment with clonazepam, 3 mg/kg of dextromethorphan per day, and sodium benzoate with doses up to 750 mg/kg per day that resulted in plasma glycine levels dropping to less than 200 μM,

From the Departments of Pediatrics (Drs. Van Hove and Jaeken) and Radiology (Dr. Demaerel), University Hospital Gasthuisberg, Leuven, Belgium; the Departments of Pediatrics (Drs. Van Hove, Kishnani, and Kahler) and Radiology (Dr. Miller), Duke University Medical Center, Durham, NC; the Victorian Clinical Genetics Services (Dr. Kahler), The Murdoch Institute, Parkville, VIC, australia; and the Department of Neurology (Dr. Rutledge), University of Alabama at Birmingham, AL.

Address correspondence and reprint requests to Dr. Johan L.K. Van Hove, Department of Pediatrics, University Hospital Gasthuisberg, Herestraat 49, B-3000 Leuven, Belgium.

 Copyright © 2000 by the American Academy of Neurology

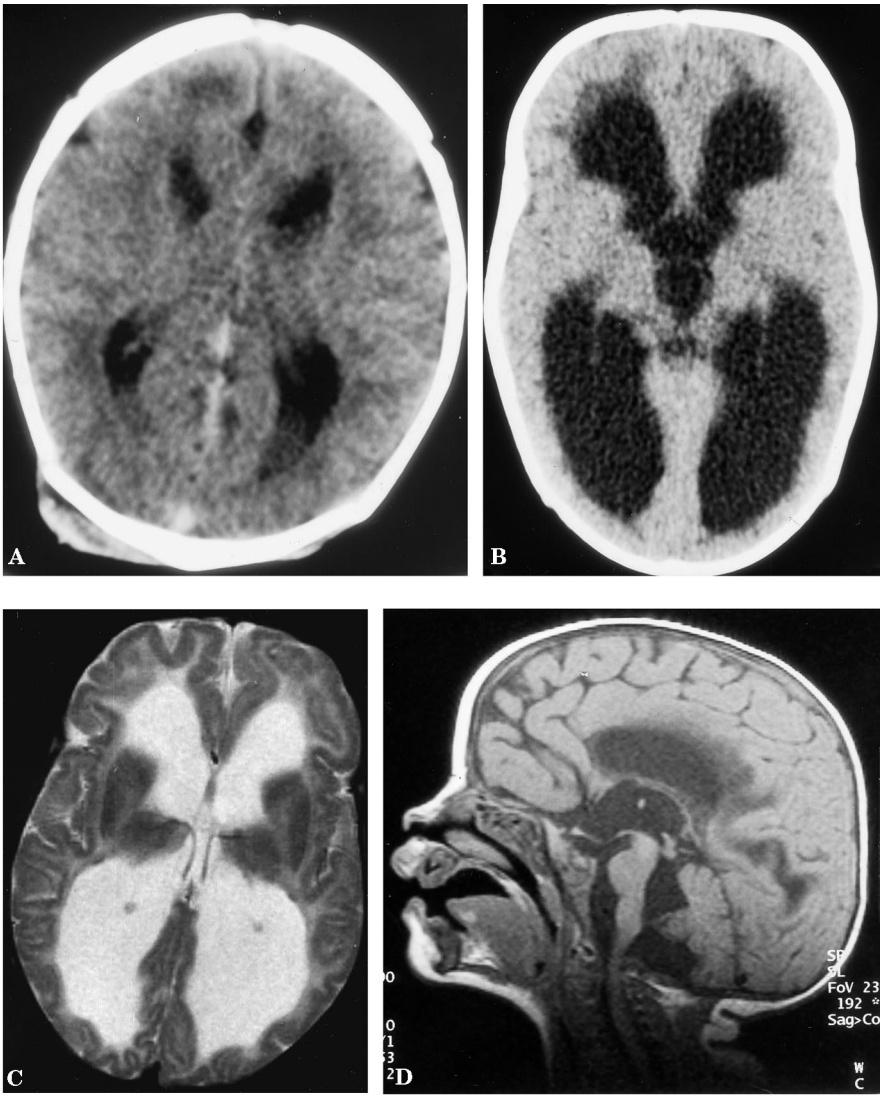

Figure. CT scan of Patient 1 taken in the first week of life (A), CT scan taken at age 4½ months at the time of the hydrocephalus (B), and MRI imaging after shunting at age 5 months in the axial (C) and sagittal plane (D).

there was improved seizure control and increased alertness. At age 4 months, he showed increased irritability, lethargy, poor sucking, and a bulging anterior fontanel. The head circumference had increased to well above the 95th percentile. Plasma glycine was 90 μM, CSF glycine 35 μM, with a CSF to plasma ratio of 0.39. Imaging by CT scan revealed massively dilated ventricles, and a significant increase in size of the posterior fossa cyst, compatible with a Dandy Walker malformation. A ventriculoperitoneal shunt was placed. During the following years, head circumference stabilized and progressively decreased to below the 3rd percentile at age 5 years. At 1 year of life, MRI revealed nearly complete absence of myelination in addition to the previously described CT abnormalities. These abnormalities persisted on follow-up. At age 5½ years, he was profoundly retarded, functioning at a developmental level of three months, with social interactive skills at the 6 month level. Plasma glycine levels have always been in the 100 to 200 μM range. He has required multiple anticonvulsants.

Case 3. This baby developed seizures and lethargy on the first day of life. Laboratory results included a plasma glycine level of 772 μM, a CSF glycine level of 167 μM, with a CSF to plasma glycine ratio of 0.21. Urine organic acids were normal. Lymphoblast glycine cleavage enzyme activity was absent. She was treated with 8.4 mg/kg of dextromethorphan per day and up to 480 mg/kg of sodium benzoate per day. Plasma glycine levels were 500 to 550 μM. She did not progress developmentally. At age 5½ months, the head size had increased from the 25th percentile over two months to the 95th percentile. Brain MRI showed ventriculomegaly affecting all ventricles with transependymal transit of fluid, and loss of gyral and sulcal markings. There was a large retrocerebellar posterior fossa cyst. The corpus callosum was present but extremely thin. A ventriculoperitoneal shunt was placed at age 8½ months with decreased irritability and stabilization of the head circumference at the 75th to 90th percentile. Computed tomography revealed continued ventricular enlargement, more prominent gyral and sulcal markings, and a posterior fossa cyst. Long-term follow-up showed persistence of ventriculomegaly. At age 4½ years, developmental outcome was poor. She smiled and occasionally laughed, but had little reaction to the environment. Although she was able to roll over, she had very poor head control and could not sit. Medications included diazepam, benzoate, and dextromethorphan.

Case 4. This boy became jittery within minutes of birth followed by progressive lethargy proceeding to coma,

requiring intubation on day two. Electroencephalogram revealed a burst suppression pattern. The CSF glycine was 247 μM, with a CSF to plasma ratio of 0.20, confirming the diagnosis of NKH. He has been treated with 4.8 mg/kg of dextromethorphan per day and 500 mg/kg of benzoate per day. At 1 month of age, a head CT revealed moderately large ventricles and a slightly prominent cisterna magna. Head circumference was at the 75th percentile. At 2 months of age, he showed obtundation, forced downward deviation of the eyes, a bulging fontanel, and increased head circumference to above the 98th percentile. A CT scan revealed massive enlargement of supratentorial ventricles, effacement of the sulci and cisterns, and a megacisterna magna. A ventriculoperitoneal shunt was placed. At 3 months, head circumference stabilized at the 98th percentile. He had no interaction with his environment. Seizures were well controlled. He was fed by gastrostomy due to severe aspiration.

Discussion. In all four patients, acute hydrocephalus occurred between ages of 2 to 6 months, requiring urgent ventriculoperitoneal shunting. Hydrocephalus had not been reported previously in NKH. Hydrocephalus presented with increasing irritability, increased seizures, papilledema, and increasing head size to greater than the 95th percentile. It involved the supratentorial ventricles in two patients, and all four ventricles in two patients. There was no increase in extra axial spaces to suggest impaired resorption of CSF by the arachnoid granulations. All four patients had a large retrocerebellar cyst that had not been noted before the acute hydrocephalus. The association of the large posterior fossa cystic malformation with obstructive hydrocephalus suggests a decompensation of a preexisting developmental malformation. The temporal relationship of the development of hydrocephalus and enlargement of the posterior fossa cyst suggests a possibly causal relationship.

Thin or absent corpus callosum has been reported in NKH as early as the first week of life.[3,4] Pathology has shown cystic myelinopathy and gliosis,[6,7] a usual preservation of gray matter,[7] and a loss of Purkinje cells and granular neurons in the cerebellum.[8,9] Magnetic resonance studies have shown absent or delayed myelination, its degree unrelated to CSF glycine levels.[3] In a few patients, gyral malformations or cerebellar hypoplasia were reported.[4] In our patients, we did not see gyral malformations, but the corpus callosum was very thin to nearly absent, and myelination was strikingly delayed to absent in all. The mild ventricular dilatation on the third day of life in Patient 1 suggests abnormalities occur very early.

All four patients were severely affected with NKH, presenting neonatally and having a high CSF to plasma glycine ratio (>0.2). There were no other known predisposing factors for the development of hydrocephalus. The plasma level of glycine varied from very low (Patient 1) to elevated (Patients 2 and 3) without correlation with the development of hydrocephalus. Medications shared by our patients included sodium benzoate and dextromethorphan, in widely varying doses. None of these medications has been previously reported to be associated with hydrocephalus in human patients. Recently, a fetal neurotoxic effect of dextromethorphan was reported in avian embryos.[10] It is possible, though unlikely, that an agent with potential fetal neurotoxicity such as dextromethorphan, may enhance the already present cerebellar atrophy[8,9] and contribute to the development of the posterior fossa abnormalities.

Outcome was very poor in all patients. There was profound mental retardation at the most severe end of the spectrum seen in NKH. Even after shunting, the ventricles remained significantly enlarged despite there being no evidence of increased pressure. Myelination was nearly absent in these regions. Marked brain atrophy was previously only reported in patients more than 1 year of age, and never in such young infants.[3] Our three older patients had severe visual impairment consistent with absent myelination of the optic radiation. In conclusion, these findings suggest that the development of acute hydrocephalus in patients with NKH is associated with a dismal prognosis.

Acknowledgment

The authors thank the many physicians sharing the care for these complex patients.

References

1. Hamosh A, Maher J, Bellus GA, Rasmussen SA, Johnston MV. Long-term use of high-dose benzoate and dextromethorphan for the treatment of nonketotic hyperglycinemia. J Pediatr 1998;132:709–713.
2. Boneh A, Degani Y, Harari M. Prognostic clues and outcome of early treatment of nonketotic hyperglycinemia. Pediatr Neurol 1996;15:137–141.
3. Press GA, Barshop BA, Haas RH, Nyhan WL, Glass RF, Hesselink JR. Abnormalities of the brain in nonketotic hyperglycinemia: MR manifestations. Am J Neuroradiol 1989;10:315–321.
4. Dobyns WB. Agenesis of the corpus callosum and gyral malformations are frequent manifestations of nonketotic hyperglycinemia. Neurology 1989;39:817–820.
5. Van Hove JLK, Kishnani P, Muenzer J, et al. Benzoate therapy and carnitine deficiency in non-ketotic hyperglycinemia. Am J Med Genet 1995;59:444–453.
6. Brun A, Borjeson M, Sjoblad S, Akesson H, Litwin E. Neonatal non-ketotic hyperglycinemia. A clinical, biochemical and neuropathological study including electronmicrocopic findings. Neuropädiatr 1979;10:195–205.
7. Trauner DA, Page T, Greco C, Sweetman L, Kulovich S, Nyhan WL. Progressive neurodegenerative disorder in a patient with nonketotic hyperglycinemia. J Pediatr 1981;98:272–275.
8. Agamanolis DP, Potter JL, Lundgren DW. Neonatal glycine encephalopathy: biochemical and neuropathologic findings. Pediatr Neurol 1993;9:140–143.
9. Shuman R, Leech RW, Scott CR. The neuropathology of the nonketotic and ketotic hyperglycinemias: three cases. Neurology 1978;28:139–146.
10. Andaloro VJ, Monaghan DT, Rosenquist TH. Dextromethorphan and other N-methyl-D-aspartate receptor antagonists are teratogenic in the avian embryo model. Pediatr Res 1998; 43:1–7.

Recombinant calcium channel is recognized by Lambert–Eaton myasthenic syndrome antibodies

Article abstract—The authors studied sera from 36 patients with Lambert–Eaton myasthenic syndrome (LEMS) by immunoblots using the recombinant protein derived from the DNA sequence encoding for the domain III S5-S6 linker of the P/Q-type voltage-gated calcium channel α1 subunit. The results of 18 patients were positive for antibodies to this recombinant protein. The results of 2 of 10 patients with lung cancer without LEMS were also positive.
Key words: Lambert–Eaton myasthenic syndrome—Neuromuscular transmission—P/Q-type voltage-gated calcium channel—Autoimmunity—Small-cell lung carcinoma.

NEUROLOGY 2000;54:757–759

Kazuo Iwasa, MD; Masaharu Takamori, MD; Kiyonobu Komai, MD; and Yasuo Mori, PhD

Lambert–Eaton myasthenic syndrome (LEMS) is an autoimmune disorder of neuromuscular transmission in which the antibodies directed against voltage-gated calcium channels (VGCCs) in the motor nerve terminals impair the presynaptic function as characterized by reduced quantal release of acetylcholine. Among the subtypes of VGCC, the current research for LEMS has focused attention on the P/Q type, against which patients with LEMS carry specific antibodies.[1,2] We previously have searched for the antigenic sites in the VGCC molecular structure through the use of synthetic peptides corresponding to various sites of the α1 subunit of P/Q-type VGCC (α1A subunit)[3] and have proposed the extracellular loops (S5-S6 linkers) of domains II and IV as potential epitopes of LEMS antibodies.[4] Although the domain III peptide was not shown to be antigenic for the detection of LEMS antibodies in our previous study,[4] this domain contains the most important amino acid sequences determining the Ca^{2+}-selectivity, Ca^{2+}-permeability, and ligand-binding ability of VGCC.[5-7] The failure in antibody detection by the domain III peptide may be caused by difficulty in inducing the peptide's antigenic conformation, which is recognized by autoantibodies raised against a native protein. Taking this possibility into consideration, we tested LEMS sera by immunoblots using the recombinant domain III protein as an antigen.

Patients and methods. Serum samples were obtained from 36 patients with LEMS whose diagnosis had been made on the basis of standard clinical and electrophysiologic criteria.[8] Seventeen patients had histologically proven small-cell lung carcinoma (SCLC). The remaining 19 patients with LEMS had no carcinoma detected over the 2 or more years' follow-up study. Serum was also collected from 10 patients with SCLC without LEMS, 5 myasthenia gravis patients with thymoma and 5 without thymoma, and 10 normal controls.

To produce the recombinant protein of the domain III (S5-S6 linker) of the P/Q-type VGCC α1 subunit in *Escherichia coli*, the open reading frame cDNA sequence encoding the domain III S5-S6 linker of the P/Q type VGCC α1 subunit (rabbit brain)[3] was amplified by PCR using sense, 5′CGGATCCAAGGGCAAGTTTTTTTCACTGCACC3′, and antisense, 5′CGCGGCCGCCTCCATGCGGTAGCCGGGGTC3′; then oligonucleotide primers were ligated with a pGEX-4T-3 vector (designed to include glutathione-s-transferase, GST). The recombinant plasmid was transformed into *E. coli* (BL21) and propagated in Lurica broth in the presence of ampicillin for the selection of the cells transformed with the pGEX-4T-3/domain III S5-S6 linker expression plasmid. To produce a GST control protein, the pGEX-4T-3 vector that did not ligate the primer was transformed into *E. coli* (BL21).

To probe with antibodies by immunoblots, the fusion protein and GST control protein were separated by 12.5% sodium dodecyl polyacrylamide gel electrophoresis, electrophoretically transferred to a polyvinylidene difluoride membrane, and incubated with serum (1:100 dilution in 3% bovine serum albumin type V with 0.05% Tween-20) or polyclonal antibodies (1:5000 dilution) that had been raised in a Lewis rat against the peptide synthesized corresponding to the domain III S5-S6 linker of the P/Q-type VGCC α1 subunit[9] or mouse anti-GST monoclonal antibody (Sigma; St. Louis, MO) (1:5,000 dilution). The sample was then incubated with horseradish peroxidase-conjugated antihuman immunoglobulin G (IgG) or antirat IgG or antimouse IgG.

The detail of the assay method for the anti-P/Q-type VGCC antibodies was reported previously.[4] The results were expressed as picomoles of ^{125}I-ω-conotoxin MVIIC-binding sites (toxin-bound human cerebellar extract) precipitated per liter of serum. Antibody titers were determined as positive when values were >3 SD above normal values for the 15 normal controls (<14.1 pmol/L).

Results. In the immunoblot of the bacterial protein expressing the domain III S5-S6 linker of the P/Q-type VGCC α1 subunit, 18 (7 with SCLS) (50%) of 36 LEMS sera and 2 (20%) of 10 SCLC sera gave staining results

From the Department of Neurology (Drs. Iwasa and Komai), Kanazawa University School of Medicine, Kanazawa; Neurological Center (Dr. Takamori), Kanazawa-Nishi Hospital, Kanazawa; and the Department of Information Physiology (Dr. Mori), National Institute for Physiological Sciences, Okazaki, Japan.

Supported by grants from the Ministry of Education, Science and Culture of Japan (No. 7457154) and the Neuroimmunological Disease Research Committee of the Ministry of Health and Welfare of Japan.

Presented in part at the Symposium of the IXth International Congress on Neuromuscular Disease; Adelaide, Australia; August 30–September 4, 1998.

Received June 11, 1999. Accepted in final form September 18, 1999.

Address correspondence and reprint requests to Dr. Masaharu Takamori, Neurological Center, Kanazawa-Nishi Hospital, 77, Ko, Kita-machi, Kanazawa, Ishikawa 920-0055 Japan.

Copyright © 2000 by the American Academy of Neurology

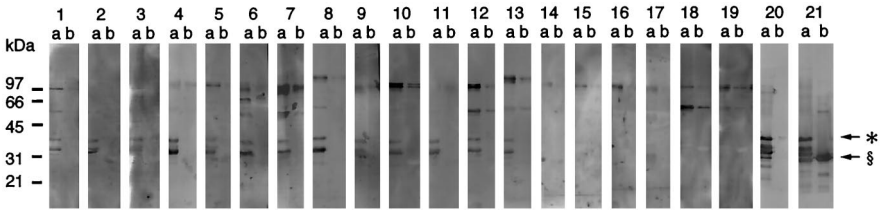

Figure 1. Immunoblot analysis of the bacterial protein with sera from patients with Lambert–Eaton myasthenic syndrome (LEMS). In each of the numbered lanes, a is a Western blot of the purified recombinant glutathione-s-transferase (GST)-P/Q-type voltage-gated calcium channel (VGCC) α1 subunit (α1A subunit) domain III S5-S6 linker fusion protein from Escherichia coli *transformed with the pGEX-4T-3 as well as the recombinant plasmid; b is a Western blot of the GST protein obtained from* E. coli *transformed with the original vector. Lanes 1 through 8: sera from anti-P/Q-type VGCC antibody-positive patients with LEMS with small-cell lung carcinoma (SCLC) reacted against the recombinant GST-domain III S5-S6 linker protein; lanes 9 through 13: sera from anti-P/Q-type VGCC antibody-positive patients with LEMS without SCLC reacted against the recombinant GST-domain III S5-S6 linker protein; lanes 14 and 15: sera from anti-P/Q-type VGCC antibody-positive patients with LEMS with SCLC did not react against the recombinant GST-domain III S5-S6 linker protein; lanes 16 through 19: sera from anti-P/Q-type VGCC antibody-negative patients with LEMS did not react with the GST-domain III S5-S6 linker protein; lane 20: rat serum containing anti-P/Q-type VGCC domain III S5-S6 linker polyclonal antibodies[9] reacted against the 39-kd protein, indicating the immune reaction with GST-P/Q-type VGCC domain III S5-S6 linker fusion protein. Bands at the migration positions of 34 kd, 32 kd, and 29 kd may represent proteolytic fragments of the 39-kd protein; lane 21: mouse anti-GST monoclonal antibody reacted against GST-fusion protein and GST protein. Molecular mass markers in kilodaltons are shown on the right. *GST-P/Q-type VGCC domain III S5-S6 linker fusion protein; §GST protein.*

that showed a 39-kd band at the same migration position as that probed with the rat polyclonal antibody to the domain III S5-S6 linker peptide and the mouse anti-GST monoclonal antibody (figures 1 and 2). These sera did not react with the GST control protein at the position probed with the anti-GST monoclonal antibody (figure 1). No reactivity was observed for immunoblots with the 39-kd protein and the GST control protein in sera from the remaining 18 patients with LEMS (figure 1), the remaining 8 patients with SCLC (figure 2), the 10 patients with myasthenia gravis (data not shown), and the 10 normal controls (data not shown).

Rat sera against an irrelevant antigen (keyhole limpet hemocyanin)[9] did not react with either the recombinant domain III protein or the GST control protein (data not shown). When the sera of patients with LEMS that were reactive with the 39-kd protein were preincubated with the recombinant domain III protein, they did not bind to the 39-kd protein on immunoblot (data not shown). Conversely, when the 39-kd protein-reactive sera from patients with LEMS were preincubated with the GST control protein, they bound to the 39-kd protein (data not shown).

Serum samples assayed against the recombinant protein were also studied by the immunoprecipitation assay for antibodies to ω-conotoxin MVIIC-sensitive P/Q-type VGCC, for which the results of 32 (89%) of the 36 patients with LEMS were positive. All 18 patients with LEMS whose results were positive for the antibody to the recombinant domain III S5-S6 linker protein were also positive for the anti-P/Q-type VGCC antibodies. The results of 4 of the 18 patients with LEMS whose results were negative for the antirecombinant domain III protein antibody also were negative for anti-P/Q-type VGCC antibodies. The results of 10 patients with SCLC, including 2 patients whose results were positive for the antirecombinant domain III protein, were negative for antibodies to P/Q-type VGCC, as were the results of 10 patients with myasthenia gravis and 10 normal controls.

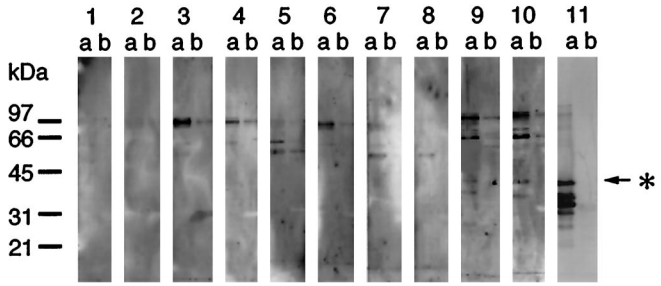

Figure 2. Immunoblot analysis of the bacterial protein with sera from 10 patients with small-cell lung carcinoma (SCLC). The pair labeled as a and b in each numbered lane corresponds to the pair in figure 1. Sera from two patients with SCLC without Lambert–Eaton myasthenic syndrome reacted against the 39-kd protein and glutathione-s-transferase control protein (lanes 9 and 10). Lane 11 corresponds to Lane 20 in figure 1.

Discussion. The α1 subunit of VGCC, which is responsible for voltage-gating, ion conduction, and sensitivity to phamacologic agents, possesses four repeated domains (I–IV), each containing six transmembrane segments (S1–S6).[7] The loop, SS1–SS2, between segments S5 and S6 in each domain is implicated in the formation of Ca^{2+}-conduction pore and is exposed extracellularly[7]; the SS2 segment of all four domains that contain glutamate residues is an important determinant of ion selectivity in the Ca^{2+} channel.[6,7] Domain III has the highest Ca^{2+} affinity[6] as well as the highest ligand-binding ability.[5] In our previous study, however, we failed to detect LEMS antibodies when the domain III S5-S6 linker synthetic peptide was used as an antigen, whereas the domain II and IV peptides were antigenic for the detection of LEMS antibodies.[4] This failure may derive from the peptide conformation. In fact, the domain III S5-S6 linker peptide used in our previous study contains many lysine residues that

tend to bind to the Bolton–Hunter reagent used for the antibody assay, so that the peptide may not effectively assume an antigenic conformation recognized by autoantibodies. The recombinant protein used in the current study resolved this matter, resulting in a 50% positivity for reaction with LEMS antibodies.

Lang et al.[10] showed through the use of cells transfected with the genes for subunits of VGCC subtypes that Ca^{2+} influx through the lines expressing the P/Q-type VGCC $\alpha 1$ subunit is specifically affected by LEMS antibodies, whereas other VGCC subtypes are not affected. The current study, as well as our previous study using synthetic peptides,[4] further clarified the target of LEMS antibodies in the P/Q-type VGCC structure at the molecular level.

Our finding that 2 of 10 patients with SCLC without LEMS have antirecombinant domain III protein antibodies is in consonance with the report that 13 of 71 patients with SCLC without LEMS have antibodies to the ω-conotoxin MVIIC-bound cerebellar extract (P/Q-type VGCC).[1] Our two patients whose results were positive for antirecombinant domain III protein antibodies had negative results for anti-P/Q-type VGCC antibodies. Thus, in some patients with SCLC, immunoblotting using the recombinant protein may be more useful in detecting the antibody rather than immunoprecipitation assay using the toxin-bound antigen.

References

1. Lennon VA, Kryzer TJ, Griesmann GE, et al. Calcium-channel antibodies in the Lambert–Eaton syndrome and other paraneoplastic syndromes. N Engl J Med 1995;332:1467–1474.
2. Motomura M, Lang B, Johnston I, Palace J, Vincent A, Newsom–Davis J. Incidence of serum anti-P/Q-type and anti-N-type calcium channel autoantibodies in the Lambert–Eaton myasthenic syndrome. J Neurol Sci 1997;147:35–42.
3. Mori Y, Friedrich T, Kim M-S, et al. Primary structure and functional expression from complementary DNA of a brain calcium channel. Nature 1991;350:398–402.
4. Takamori M, Iwasa K, Komai K. Antibodies to synthetic peptides of the α1A subunit of the voltage-gated calcium channel in Lambert–Eaton myasthenic syndrome. Neurology 1997;48:1261–1265.
5. Ellinor PT, Zhang J-F, Horne WA, Tsien RW. Structural determinants of the blockade of N-type calcium channels by a peptide neurotoxin. Nature 1994;372:272–275.
6. Ellinor PT, Yang J, Sather WA, Zhang J-F, Tsien RW. Ca^{2+} channel selectivity at a single locus for high-affinity Ca^{2+} interactions. Neuron 1995;15:1121–1132.
7. Varadi G, Mori Y, Mikala G, Schwartz A. Molecular determinants of Ca^{2+} channel function and drug action. Trends Pharmacol Sci 1995;16:43–49.
8. O'Neill JH, Murray NM, Newsom–Davis J. The Lambert–Eaton myasthenic syndrome. A review of 50 cases. Brain 1988;111:577–596.
9. Komai K, Iwasa K, Takamori M. Calcium channel peptide can cause an autoimmune-mediated model of Lambert–Eaton myasthenic syndrome in rats. J Neurol Sci 1999;166:126–130.
10. Lang B, Waterman S, Pinto A, et al. The role of autoantibodies in Lambert–Eaton myasthenic syndrome. Ann NY Acad Sci 1997;841:596–605.

Neurogenic stunned myocardium in Guillain–Barré syndrome

Article abstract—Neurogenic stunned myocardium (NSM), a syndrome of reversible left ventricular dysfunction best described after subarachnoid hemorrhage, has not been associated with peripheral neuropathy. We describe a woman with Guillain–Barré syndrome in whom a syndrome compatible with NSM developed in the setting of a physiologically documented increase in sympathetic cardiovascular tone. This case supports the presumed unifying role of excessive sympathetic nervous system activation in the pathogenesis of NSM. **Key words:** Neurogenic stunned myocardium—Guillain–Barré syndrome—Electrocardiogram—Echocardiography.

NEUROLOGY 2000;54:759–762

Richard Bernstein, MD, PhD; Stephan A. Mayer, MD; and Anthony Magnano, MD

Neurogenic stunned myocardium (NSM) is a syndrome of reversible left ventricular (LV) dysfunction and mild creatine kinase myocardial isoenzyme (CK-MB) elevation that occurs after severe CNS injury in the absence of coronary artery disease.[1,2] NSM is best described after aneurysmal subarachnoid hemorrhage (SAH); it occurs in approximately 5% of cases and is associated with poor clinical grade (Hunt/Hess grades III-V) and female gender.[2] In severe cases, hypotension, reduction of cardiac output, and coexisting neurogenic pulmonary edema can occur.[2] Characteristic electrocardiographic (ECG) findings of NSM in patients with SAH include deep, symmetric T-wave inversions and severe QT segment prolongation.[1] By contrast, other ECG abnormalities associated with SAH, although common and varied, usually are clinically insignificant.

The pathophysiology of NSM is controversial. Pathologically, 50% of patients with fatal SAH show myocardial contraction band necrosis.[1] Other condi-

From the Division of Critical Care Neurology, Department of Neurology, Neurological Institute (Drs. Bernstein and Mayer); and the Division of Cardiology, Department of Medicine (Dr. Magnano), Columbia-Presbyterian Medical Center, New York, NY.

Received June 14, 1999. Accepted in final form September 22, 1999.

Address correspondence and reprint requests to Dr. Stephan A. Mayer, Division of Critical Care Neurology, Neurological Institute, 710 West 168th Street, Box 39, New York, NY 10032.

Copyright © 2000 by the American Academy of Neurology

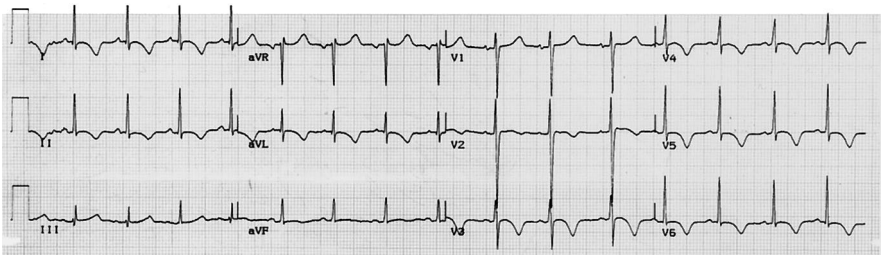

Figure. Twelve-lead electrocardiogram performed on the 3rd hospital day and 10th day of illness showing diffuse symmetric T-wave inversion in leads I, II, aVL, and V1–V6 and severe QTc prolongation (0.473 second).

tions in which reversible cardiac dysfunction has been associated with contraction band necrosis include head trauma,[3] pheochromocytoma,[4] fatal status asthmaticus,[5] sudden death associated with violent assault,[3] and brain death[1] (reviewed in reference 3). These clinical associations, and experimental studies in which contraction band necrosis has been produced by catecholamine infusion and autonomic discharges associated with direct CNS stimulation,[3] implicate excessive sympathetic outflow and catecholamine toxicity in the pathogenesis of NSM.[1,3]

Cardiac rhythm disturbances and morphologic ECG changes are well-described in Guillain–Barré syndrome (GBS) and result from involvement of the autonomic nervous system in the neuropathic process. Similar to aneurysmal SAH, widespread, deep T-wave inversions with prolonged QTc intervals have been observed with GBS.[6] Labile blood pressure, including profound hypotension, has also been described in GBS,[7] but LV dysfunction similar to that seen with severe CNS injury has not been documented. We describe a patient with GBS with electrophysiologic evidence of increased sympathetic tone in whom reversible LV dysfunction, characteristic ECG changes, and mild CK-MB elevation developed, which is consistent with NSM.

Case report. A previously healthy 29-year-old woman who was 7 weeks' postpartum presented with a 1-week history of cramping in the feet followed by mild, symmetric arm and leg weakness, dysphagia, and dysarthria. There were no antecedent illnesses. On initial examination, her heart rate was 80, her blood pressure was 130/80, and she was afebrile. There was no bulbar or respiratory weakness. She had distal four of five weakness of both hands and of the proximal and distal leg muscles. There was diminished vibratory sensation at the toes bilaterally. Deep tendon reflexes could not be elicited, and the plantar reflexes were flexor. The CSF had an elevated protein (68 mg/dL) and was acellular. Nerve conduction studies showed prolonged distal latencies, slow conduction velocities, and evidence of conduction block; needle electromyogram showed scattered fibrillations and decreased recruitment.

The clinical diagnosis was GBS. She was treated with 2 g/kg of IV immunoglobulin over 5 days, followed by 18 L of plasma exchange over 5 days. During this period, her weakness progressed to flaccid quadraparesis with respiratory compromise, and she was electively intubated on the 5th hospital day, corresponding to the 12th day of her illness. By the 15th hospital day, she was extubated and her limb strength had improved. However, on the 19th hospital day, further respiratory compromise developed and she was reintubated. Repeat CSF examination showed a protein of 76 mg/dL and 1 white blood cell/μL. Repeat nerve conduction studies showed prolonged motor distal latencies, increased temporal dispersion, absent F waves, absent sensory responses, and acute denervation in the legs, consistent with a demyelinating motor sensory neuropathy with secondary axonal loss. A repeat course of plasmapheresis corresponded with improved strength, although her legs remained severely weak. Results from a motor and sensory nerve biopsy showed myelin breakdown, consistent with GBS. Etiologic investigations, including HIV, Epstein–Barr virus, varicella zoster virus, herpes simplex virus type-1 and type-2, cytomegalovirus, anti-extractable nuclear antigen, anti-DNA, anti-sulfatide, anti-GM1, anti-MAG, anti-Gd1b, anti-Gq1b, and anti-HU titers were all normal or negative, as were test results of CSF cytology, CSF Lyme titer, thyroid function, angiotensin-converting enzyme level, serum quantitative immunoglobulin, c-ANCA, urine heavy metal and porphobilinogen levels, and cryoglobulins. Antinuclear antibody was positive to 1:40 with a speckled pattern, and the antihepatitis-B core antibody was positive, although liver enzymes were normal.

Before her neurologic illness, she had no known cardiac disease or symptoms and no risk factors for heart disease. Her ECG on admission was normal, with a rate of 70 and no evidence of ischemia. However, on the third hospital day, when her neurologic status acutely worsened, sinus tachycardia developed to a maximum of 120 beats per minute. An ECG showed diffuse, symmetric T-wave inversions in leads I, II, avL, and V1-V6 and a QTc of 0.473 second (figure). A transesophageal echocardiogram performed the following day showed apical akinesis and diffuse LV hypokinesis with a severely reduced ejection fraction (25%). There was no associated hypotension. On the same day, serum creatine kinase was 245 U/L (normal, 39–238) with 2.7% segregating as CK-MB (normal, <2.0%), serum epinephrine was 880 pg/mL (normal, 110–410), and a 24-hour Holter monitor showed severely reduced heart rate variability with a mean cardiac cycle length of 530 ± 32 msec (normal, 141 ± 39 msec). Twenty-four-hour power spectral analysis showed severely reduced high-frequency power (20.5 $msec^2$; normal, 975 ± 203 $msec^2$) consistent with parasympathetic withdrawal, and the ratio of low-frequency to high-frequency power was consistent with a shift in sympathovagal balance toward sympathetic predominance (3.75; normal, 1.5–2).[8] By hospital day 9, the T-wave inversions had resolved, although she remained tachycardiac. A repeat echocardiogram on hospital day 24 showed a normal ejection fraction with no

regional or global wall motion abnormalities. There were no further cardiac complications.

Discussion. We describe for the first time a case of acute neuropathy complicated by reversible LV dysfunction, which was presumably neurogenic in origin. Our patient, a healthy young woman, had no history or signs of cardiac dysfunction on her initial presentation. Early in the course of what proved to be a severe demyelinating polyneuropathy requiring mechanical ventilation, a diffuse, symmetric T-wave inversion and QTc prolongation developed, ECG changes that have been correlated with LV dysfunction after SAH.[1] There was mild elevation of serum CK-MB and echocardiographic evidence of both segmental and global LV hypokinesis. Follow-up ECG and echocardiography 3 weeks later showed that the entire syndrome had resolved. The rapid onset and resolution of the syndrome, the characteristic ECG and echocardiographic changes, the association of the syndrome with an acute, severe neurologic illness, and the absence of other identifiable cardiac risk factors in an otherwise healthy young woman fulfill the criteria for NSM.[1,3]

One potential problem with our interpretation of the clinical data is that the patient was 7 weeks' postpartum and had no baseline echocardiogram before the onset of her acute neuropathy. Therefore, one could argue that the wall motion abnormalities documented on her first echocardiogram might have predated the onset of her neurologic illness. However, she had no history of cardiac disease during or immediately after her pregnancy, and her ECG only began to show abnormalities as her neuropathy worsened. The CK-MB levels were only minimally elevated (which is typical of NSM),[1,2] and the syndrome resolved completely over time, which would not be expected if she had peripartum cardiomyopathy. Although we did not perform coronary angiography, we had no reason to suspect coronary artery disease in a young woman with no risk factors. Severe inflammatory myocarditis has been described in GBS[9] but is extremely rare and would be unlikely to improve over a period of weeks. Because a myocardial biopsy was not performed, the cause of the cardiac disturbance in our patient remains speculative; however, we believe the preponderance of evidence supports the diagnosis of NSM.

This report expands the range of illnesses that may produce NSM to include diseases of the peripheral nervous system and contributes to our understanding of the pathogenesis of neurogenic cardiac injury. Contraction band necrosis resulting from increased sympathetic tone and catecholamine toxicity is thought to be the pathologic substrate of NSM.[1,3] In fact, microneurographic studies have documented sympathetic hyperactivity in GBS,[10] which may reflect impaired baroreceptor modulation. Our patient showed a severe reduction in heart rate variability and a shift toward a predominantly low-frequency autonomic modulation of heart rate, consistent with increased sympathetic tone, a vagolytic effect, or both. Studies of circulating catecholamines in SAH have failed to show increased levels in patients with ECG changes, implicating direct neural stimulation, rather than systemic adrenergic secretion, in the pathogenesis of neurogenic cardiac injury.[1] Our patient had an elevated serum norepinephrine level when echocardiographic abnormalities developed. Whether elevated circulating catecholamine levels, increased sympathetic outflow via the cardiac nerves, or both caused her LV dysfunction cannot be determined from this single clinical observation.

The possibility that NSM may occur in GBS has clinical implications for the treatment of patients with dysautonomia from acute peripheral neuropathies. Dysautonomia is common in GBS, often causing profound swings in blood pressure or sustained hypotension.[6] Although this has been ascribed to dysregulation of venomotor tone or systemic vascular resistance,[6] impaired LV performance, as documented in this case, might also contribute to hypotension in GBS and should be looked for in patients with ECG changes and cardiac enzyme elevations. In our patient, the degree of cardiac dysfunction was not severe enough to cause hypotension. However, in more severely affected, older, or volume-depleted patients, a similar degree of cardiac dysfunction could lead to hemodynamic instability, as it sometimes does in SAH.[1,2] Echocardiography should be performed in patients with GBS with labile blood pressure, abnormal ECG findings, or cardiac enzyme elevations, and hemodynamic monitoring and vasopressors should be instituted as needed to prevent systemic sequelae of hypotension.

NSM may occur in patients with GBS. We hope that this report stimulates more systematic investigation of cardiac dysfunction in acute peripheral neuropathies, allowing a determination of the generalizability of this clinical problem and a fuller understanding of its pathogenesis.

References

1. Mayer SA, Swarup R. Neurogenic cardiac injury after subarachnoid hemorrhage. Curr Opin Anesthesiology 1996;9:356–361.
2. Mayer SA, Lin J, Homma N, et al. Myocardial injury and left ventricular performance after subarachnoid hemorrhage. Stroke 1999;30:780–786.
3. Samuels, MA. "Voodoo" death revisited: the modern lessons of neurocardiology. The Neurologist 1997;3:293–304.
4. Elian D, Harpaz D, Sucher E, Kaplinsky E, Motro M, Vered Z. Reversible catecholamine-induced cardiomyopathy presenting as acute pulmonary edema in a patient with pheochromocytoma. Cardiology 1993;83:118–120.
5. Drislane FW, Samuels MA, Kozakewich H, Schoen FJ, Strunk R. Myocardial contraction bands lesions in patients with fatal asthma: possible neurocardiologic mechanisms. Am Rev Resp Dis 1987;135:498–501.
6. Greenland P, Griggs RC. Arrhythmic complications in the Guillain–Barré syndrome. Arch Intern Med 1980;140:1053–1055.
7. Ropper AH, Wijdicks EFM. Blood pressure fluctuations in the dysautonomia of Guillain–Barré syndrome. Arch Neurol 1990;27:337–338.
8. Task Force of the European Society of Cardiology and the North American Society of Pacing and Electrophysiology.

Heart rate variability: standards of measurement, physiological interpretation and clinical use. Circulation 1996;93:1043–1065.
9. Hodson AK, Hurwitz BJ, Albrecht R. Dysautonomia in Guillain–Barré syndrome with dorsal root ganglionopathy, Wallerian degeneration, and fatal myocarditis. Ann Neurol 1984;15:88–95.
10. Fagius J, Wallin BG. Microneurographic evidence of excessive sympathetic outflow in Guillain–Barré syndrome: a test of autonomic dysfunction. Brain 1983;106:589–600.

"Tactile" sensory nerve potentials elicited by air-puff stimulation: A microneurographic study

Article abstract—To investigate the sensory nerve responses to selective touch stimulation, sensory nerve action potentials after brief air-puffs were recorded with a microelectrode. In patients with peripheral neuropathy, those with impairment of tactile sensations had significantly smaller responses than did those without tactile impairment, suggesting receptor activation failure as well as nerve conduction failure. Brief air-puff stimulation, when combined with microneurography, could be used for evaluating the tactile receptor properties in humans. **Key words:** Sensory nerve action potential—Air-puff stimulation—Microneurography—Tactile sensation.

NEUROLOGY 2000;54:762–765

S. Kuwabara, MD; K. Mizobuchi, MD; S. Toma, MD; Y. Nakajima, MD; K. Ogawara, MD; and T. Hattori, MD

Conventional surface recording of sensory nerve action potentials (SNAPs) after electric stimulation is a useful diagnostic tool in clinical practice. Electric stimulation, however, produces an artificially synchronized nerve volley, which the nervous system never normally experiences, and it bypasses the peripheral receptor. To assess the correlation between sensory symptoms and test abnormalities in patients with peripheral neuropathy, natural stimulus is required. Although mechanical stimulation techniques[1-3] have been developed, previous methods may activate underlying joint, tendon, or muscle receptors. An air-puff stimulator developed by Hashimoto et al.[4-6] can provide air-puffs with fast rising times and reproducible tactile stimuli, selectively activating cutaneous mechanoreceptors. Air-puff SNAPs have been recorded with surface electrodes,[6] but evoked responses were very small. Because recordings with a microelectrode inserted into the nerve show high signal-to-noise ratios,[7] air-puff SNAPs may be detectable even in patients with peripheral neuropathy. To investigate the characteristics of tactile SNAPs and their correlation with clinical touch sensation in patients, this study used both microneurographic techniques and an air-puff stimulator.

From the Departments of Neurology (Drs. Kuwabara, Mizobuchi, Ogawara, and Hattori) and Neurophysiology (Drs. Toma and Nakajima), Chiba University School of Medicine, Chiba, Japan.

Received April 7, 1999. Accepted in final form October 1, 1999.

Address correspondence and reprint requests to Dr. Satoshi Kuwabara, Department of Neurology, Chiba University School of Medicine, 1-8-1 Inohana, Chuo-ku, Chiba 260-8670, Japan.

Methods. *Patients.* Microneurographic recordings of SNAPs were performed in 6 normal subjects (age, 24 to 60 years) and in 13 patients with peripheral neuropathy (table). All subjects gave written, informed consent to the experimental procedures. The study had the approval of the local ethical committee.

Microneurographic recordings. A tungsten microelectrode (25-05-1; Frederik Haer Corp., Brunswick, ME) was inserted into the median nerve at the elbow and was used for recordings. Electric and air-puff stimulation was delivered to the volar surface of the fingertip in the receptive field, and 50 responses were averaged.

Air-puff and electric stimulation. Air-puffs were produced by a stimulator (Nihon-Kohden Co. Ltd., Tokyo, Japan)[4,5] and delivered at a rate of 1 Hz through a nozzle 0.6 mm in diameter placed 1 cm from the target skin surface. The stimulated cross-sectional area was 2.5 mm^2. An air-puff had a rise time of 0.5 msec and a pressure of 300 mN. SNAPs were filtered (bandpass, 500 Hz to 5 kHz) and recorded with a electromyogram machine (Viking, Nicolet Biomedical Japan, Tokyo, Japan). The Mann–Whitney test was used for statistical analysis.

Results. *Normal subjects.* When an electrode was inserted into the nerve, a receptive field was found in the territory of two to four digital nerves. Air-puff-evoked SNAPs were clearly recorded in all six subjects. Representative responses are shown in the figure. The amplitudes of the air-puff SNAPs were much smaller than those of electric SNAPs (table, bottom); they ranged from 7% to 34% of the electric SNAP amplitudes. Latencies of air-puff SNAPs were invariably longer than those of the electric SNAPs (range of difference, 0.9 to 3.4 msec). The

 Copyright © 2000 by the American Academy of Neurology

Table. *Electric and air-puff SNAPs in patients with peripheral neuropathy*

Patient no.	Diagnosis	Electric SNAP amplitude (μV)	Air-puff SNAP amplitude (μV)	Latency difference (msec)
With decreased touch sensation*				
1	Beriberi	10	NR	—
2	CIAN	20	NR	—
3	Diabetes	6.5	1.1	2.2
4	CIDP	12.4	NR	—
5	CIDP	12.1	NR	—
6	CIDP	8.1	NR	—
7	GBS	7.5	1.8	2.5
With normal touch sensation*				
1	POEMS	21.5	3.1	2.1
2	CIAN	14.5	2.1	1.6
3	Brachial plexopathy	9.5	1.9	3.5
4	HNPP	27.9	4.1	2.5
5	CIDP	30.9	4.5	3
6	GBS	51.5	3.5	1.2
Normal mean (range)		76.1 (28–120)	11.9 (6.5–27.6)	1.6 (0.9–3.4)

* In the tested finger tip.
SNAP = sensory nerve action potential; CIAN = chronic idiopathic ataxic neuropathy; CIDP = chronic inflammatory demyelinating polyneuropathy; GBS = Guillain-Barre syndrome; POEMS = organomegaly, endocrinopathy, M-protein, and skin changes; HNPP = hereditary neuropathy with liability to pressure palsy; NR = not recordable.

air-puff SNAPs were polyphasic and their duration ranged from 4.1 to 9.4 msec.

Patients with peripheral neuropathy. Representative waves are shown in the figure, and characteristics of electric and air-puff SNAPs in patients are listed in the table. Electric SNAPs were recordable in all patients, whereas air-puffs did not evoke identifiable responses in five patients, all of whom had decreased tactile sensations. Of these, three did not perceive air-puffs, and the remaining two reported noticing only subtle sensations on application of the air-puffs. Compared to normal subjects, patients had lower amplitudes of both electric ($p < 0.01$) and air-puff ($p < 0.01$) SNAPs.

In patients with impaired tactile sensations, both electric ($p = 0.02$) and air-puff SNAPs ($p = 0.003$) were smaller compared with those of patients without impaired tactile sensations. The latency difference between electric and air-puff SNAPs was similar between patients and normal subjects.

Discussion. This study showed that SNAPs after air-puff stimuli could be reliably observed with microneurography and that the amplitude of air-puff SNAPs correlated well with clinical tactile impairment. It is likely that the exact site of electric stimulation is the distal axons rather than the receptors, even if the stimulus is delivered to the skin. Because electric stimulation applied at the fingertip stimulates branches of the two digital nerves, the activity of hundreds of large myelinated fibers contributes to the electric SNAPs. In contrast, air-puff SNAPs have different characteristics. First, the number of the activated sensory units is much smaller than that observed after electric stimulation. This could explain the much smaller amplitude of air-puff SNAPs. Second, air-puff-induced responses reflect additional processes such as the rising time of the stimulus, skin indentation, receptor transduction, and possibly neural transmission in the nerve ending.

In normal subjects, the latency difference between electric and air-puff SNAPs, which ranged from 0.9 to 3.4 msec, is consistent with that in previous studies using surface electrodes (0.8 to 1.6 msec)[6] or somatosensory-evoked potentials (2 to 4 msec).[4] If sharp air-puffs can minimize the process variation of skin indentation, the differences are considered to reflect mainly the receptor transduction time. The latency difference may not accurately reflect receptor activation time because of the different population of the activated sensory units between electric and air-puff stimulation. Nevertheless, the comparison of SNAPs after the administration of two kinds of stimulus may provide information about the receptor transduction properties.

A previous surface electrode study showed that air-puff stimulation elicited two to four separate waves.[6] Our study confirmed polyphasic air-puff SNAPs in normal subjects. The mechanical threshold of individual receptors in the human glabrous hand

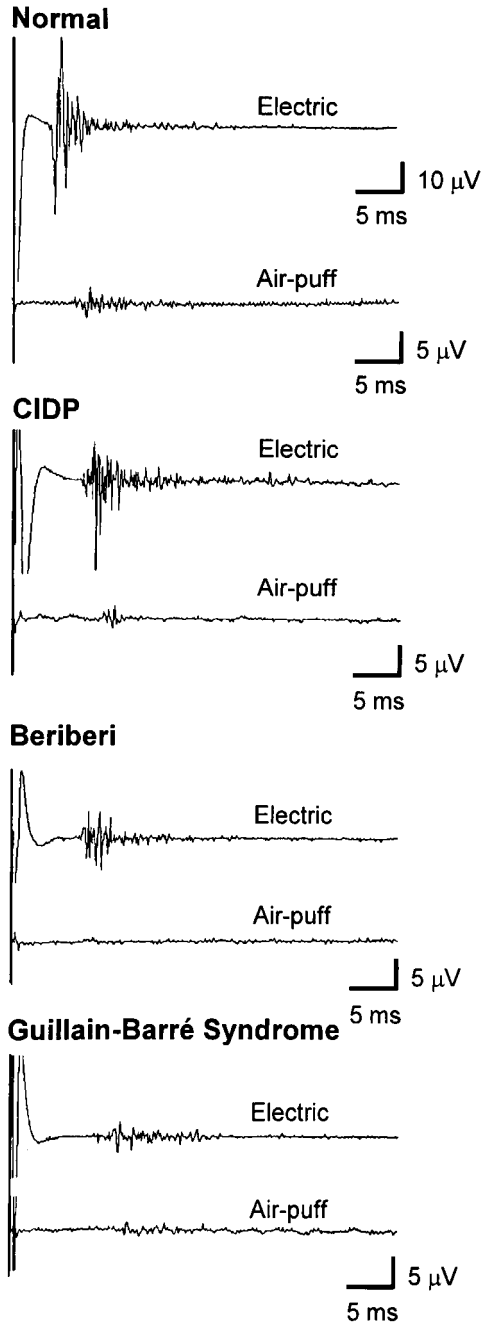

Figure. Microneurographic recordings of sensory nerve action potentials (SNAPs) after electric and air-puff stimulation in normal subjects and in patients with peripheral neuropathy. The air-puff SNAP is much smaller than electric SNAP. A patient with chronic inflammatory demyelinating polyneuropathy (CIDP) was free of sensory symptoms at the time of examination, whereas patients with beriberi neuropathy or Guillain–Barré syndrome (GBS) had moderate decreases in tactile sensation. A patient with beriberi shows no detectable air-puff SNAP despite a relatively preserved electric SNAP, whereas a patient with GBS shows proportional conduction slowing and temporal dispersion between electric and air-puff SNAPs.

is distributed over a wide range from 1 to 100 mN.[8] Median thresholds of rapidly adapting mechanoreceptors and Pacinian corpuscles were 5.8 mN and 5.4 mN, respectively, whereas slowly adapting receptors types 1 and 2 had higher thresholds (13 and 75 mN, respectively). Because the air-puffs possess a pressure of 300 mN, all four receptors could be activated. The multiple peaks of air-puff SNAPs may be caused by[1] different conduction velocities of the activated sensory units,[2] different effective sites of stimulation in units that had large receptive fields, and[3] repetitive firing of the receptor in response to single air-puff stimulus.

Air-puff SNAPs were not elicited in patients with decreased touch sensation. Such abnormalities presumably had two components, namely, receptor transduction failure and nerve conduction failure. Skin receptors are transducing elements located in the peripheral terminals. In dying-back neuropathies, the receptors are affected earlier and more severely than the intermediate segments. Thus, altered receptor properties[9,10] may be the earliest dysfunction in axonal degeneration. In our patients with beriberi, chronic idiopathic ataxic neuropathy, or diabetes, air-puff SNAPs were lost despite the presence of relatively preserved electric SNAPs (table, figure). This possibly results from receptor activation failure. Conversely, the decrease in air-puff SNAPs probably is caused by neural transmission failure in demyelinating neuropathy. Because the distal nerve segments are preferentially affected in these immune-mediated demyelinating neuropathies, the low amplitudes probably result from conduction block or temporal dispersion of the neural volley. Theoretically, receptor properties are not affected unless demyelination is associated with secondary axonal degeneration. Under such conditions, the electric and air-puff SNAPs are expected to be proportionally affected. This study showed normal receptor transduction times in patients with demyelinating neuropathy.

A low air-puff SNAP was significantly associated with impaired tactile sensations in both axonal and demyelinating neuropathies. There may exist a different pathophysiology of impaired tactile sensations involved in the two types of nerve pathology. Evaluation of tactile SNAPs would provide further insight about peripheral sensory physiology as well as about the correlation between electrodiagnostic abnormalities and symptomatology.

References

1. Larsson LE, Prevec TS. Somatosensory response to mechanical stimulation as recorded in the human EEG. Electroencephalogr Clin Neurophysiol 1970;28:162–172.
2. Ishiko N, Hanamori T, Matsuyama N. Spatial distribution of somatosensory responses evoked by tapping the tongue and finger in man. Electroencephalogr Clin Neurophysiol 1980;50: 1–10.
3. Pratt H, Starr A. Mechanically and electrically evoked somatosensory potentials in humans: scalp and neck distribution of short latency components. Electroencephalogr Clin Neurophysiol 1982;51:138–147.

4. Hashimoto I. Somatosensory evoked potentials elicited by air-puff stimuli generated by a new high-speed air control system. Electroencephalogr Clin Neurophysiol 1987;67:231–237.
5. Hashimoto I, Yoshikawa K, Sasaki M, Gatayama T, Nomura M. Conduction velocity and temporal dispersion of the nerve volleys evoked by air-puff stimulation of the index finger and palm. Electroencephalogr Clin Neurophysiol 1991;81: 102–107.
6. Hashimoto I, Yoshikawa K, Sasaki M, Gatayama T, Nomura M. Sensory nerve action potentials elicited by mechanical air-puff stimulation of the index finger in man. Electroencephalogr Clin Neurophysiol 1989;72:321–333.
7. Kuwabara S, Nagase H, Arai K, Hattori T. Slowly conducting, low-threshold components of sensory nerve potentials in peripheral neuropathy: a microneurographic study. Muscle Nerve 1997;20:961–968.
8. Johansson RS, Valbo ÅB, Wresling G. Thresholds of mechanosensitive afferents in the human hand as measured with von Frey hairs. Brain Res 1980;184:343–351.
9. Mackel R. Human cutaneous mechanoreceptors during regeneration: physiology and interpretation. Ann Neurol 1985;18: 165–172.
10. Mackel R. Properties of cutaneous afferents in diabetic neuropathy. Brain 1989;112:1359–1376.

Cortical reorganization after acute unilateral hearing loss traced by fMRI

Article abstract—Unilateral acoustic stimulation produces a functional MRI (fMRI)–blood-oxygenation-level-dependent (BOLD) response mainly in the contralateral auditory cortex. In unilateral deaf patients, the BOLD response is bilateral. We studied a subject with sudden hearing loss after cochlear nerve resection before and repeatedly after surgery. During normal bilateral hearing, contralateral cortical BOLD responses were found. Progressing compensatory reorganization with bilateral representation of unilateral stimulation was detected over a period of approximately 1 year. **Key words:** Neuronal plasticity—fMRI—Acoustic stimulation—Auditory cortex.

NEUROLOGY 2000;54:765–767

D. Bilecen, MD, PhD; E. Seifritz, MD; E.W. Radü, MD; N. Schmid, MD; S. Wetzel, MD; R. Probst, MD; and K. Scheffler, PhD

In a previous study, we showed a strong contralateral cortical representation of acoustic stimuli in normal humans by means of blood-oxygenation-level-dependent (BOLD) functional MRI (fMRI).[1] These findings were qualitatively consistent with magnetoencephalographic[2] and electrophysiologic data.[3] The cortical volume showing a BOLD signal in response to unilateral stimulation was approximately three to five times greater in the contralateral than in the ipsilateral hemisphere.[1] Binaural acoustic stimulation yielded an activation that was almost balanced between the two hemispheres. Interestingly, this was approximately one-third larger than the sum of both unilateral stimulations and suggested binaural facilitation or unilateral inhibition,[2-4] a phenomenon that is associated with sound localization in space.[5] In contrast to these physiologic findings are the data that were acquired in unilateral deaf patients. These showed an almost balanced bilateral, rather than mainly contralateral, BOLD response to monaural stimulation of the intact ear.[1] The data were in line with magnetoencephalographic studies[6] and suggested a functional reorganization of the central auditory system after unilateral damage.

In the current study, we sought to explore the development of this phenomenon over time. We had the rare opportunity to repeatedly measure the BOLD response to acoustic stimulation in an initially normal-hearing patient who had lost hearing after acoustic neurinoma resection. The patient had been studied 1 month before surgery and 1, 5, and 55 weeks after surgery.

Materials and methods. *Patient.* The patient was a right-handed 53-year-old woman. She had a right-sided cerebellopontine angle vestibular schwannoma with a diameter of 25 mm with preserved hearing level. The tumor was mainly located toward the brain stem and, to a lower extent, within the portion of the meatus acusticus. Resection through the retrosigmoid approach with attempted hearing preservation was performed by an otoneurosurgical team led by one of us (R.P.). Because of tumor location

From the Departments of Radiology (Drs. Bilecen, Radü, and Wetzel), Psychiatry (Dr. Seifritz), and Otorhinolaryngology (Drs. Schmid and Probst), University of Basel, Switzerland; and the Section of Medical Physics, Department of Diagnostic Radiology (Dr. Scheffler), University of Freiburg, Germany.

Supported in part by SNF # 31.32533.91, 32.33850.92, and 3200-052194.97. A University of Basel habilitation stipend is held (E.S.).

Received September 9, 1999. Accepted in final form October 1, 1999.

Address correspondence and reprint requests to Dr. Erich Seifritz, Department of Psychiatry, University of Basel, Psychiatric University Hospital, Wilhelm Kleinstr. 27, CH-4025 Basel, Switzerland.

Copyright © 2000 by the American Academy of Neurology

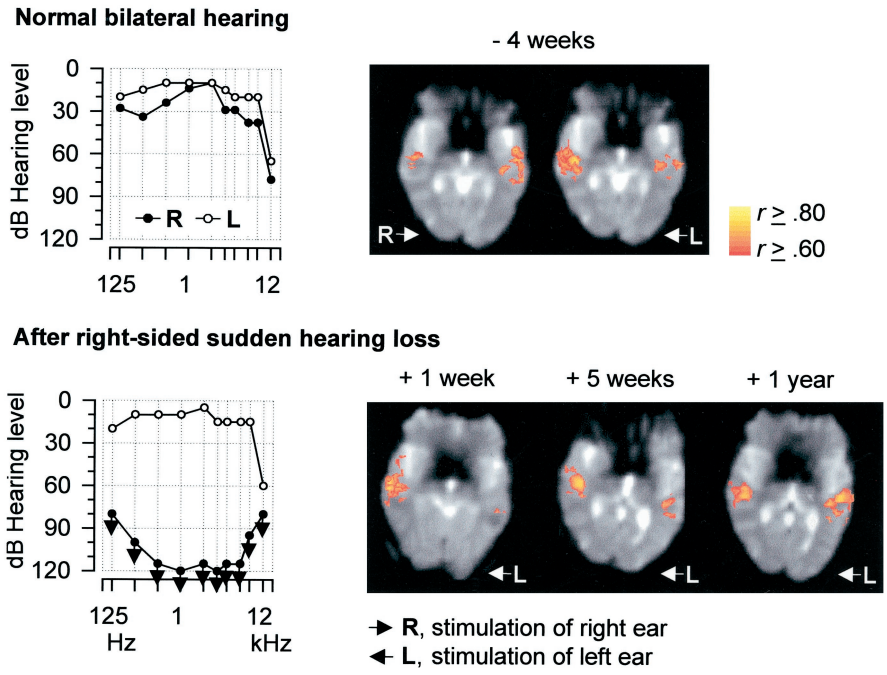

Figure. Pure-tone audiometry 1 week before and 3 months after acoustic nerve resection. Blood-oxygenation-level-dependent (BOLD) response pattern (colored pixels projected on the EPI slice in the bicommissural plane) in the primary auditory cortex after unilateral stimulations. Before surgery, a chiefly contralateral response pattern was found. After surgery, stimulation of the left ear produced a progressively more balanced bilateral rather than a contralateral BOLD response pattern.

and size, the vestibulocochlear nerve was destroyed and hearing could not be preserved (c.f. pure-tone audiometries in the figure). No other cranial nerves were damaged. One month after initial surgery, revision mastoidectomy was necessary because of CSF leakage. Other problems including meningitis were not encountered. The patient gave written, informed consent to the fMRI studies that were approved by the local ethics committee.

Imaging. Structural and fMRI data were acquired on a 1.5-tesla Magnetom VISION scanner (Siemens, Erlangen, Germany) using a standard circularly polarized head coil. Localizers were done with a T_1-weighted sequence (TE = 14 msec, TR = 300 msec). Details of the fMRI protocol have been described previously.[1] A single-shot gradient-recalled echo-planar imaging (EPI) sequence (TE = 70 msec, TR = 15 seconds) was used that allowed the acquisition of nine 4-mm slices within 1.8 seconds (field of view 250 × 219 mm, 128 × 108 matrix, seventh slice aligned in bicommissural plane). A long TR was used to disentangle experimental excitation from the excitation produced by the scanner noise. Acoustic stimulation was performed through a pneumatic system through which a 1,000-Hz sine tone (95-dB sound pressure level, pulsed with 6 Hz) was applied following a box-car design (OFF-ON-OFF-ON-OFF-ON). The patient was asked to passively listen to the tones. Acoustic stimulations during fMRI studies were performed: 1) at 4 weeks before surgery (bilateral hearing) and 2) at 1 week, 3) 5 weeks, and 4) 1 year after surgery.

Data analysis. The statistical parametric mapping software BrainVoyager 3.0 (Brain Innovation, Frankfurt/Main, Germany; http://www.brainvoyager.de) was used for data analysis. After three-dimensional motion correction, linear correlation maps were constructed. A pixel-wise correlation coefficient of $r > 0.60$ was considered statistically significant. For quantitation of the response, relative unilateral cortical activation volumes (i.e., sum of significant voxels within the slab covered by the EPI slices) were taken ("laterality").

Results *Audiometry.* As shown in the figure, pure-tone audiometry 5 days before surgery yielded almost normal bilateral hearing (left: 98%, right: 94%). In the audiometric examination on postsurgery week 12, complete right-sided deafness (left: 99%, right: 0%) was found.

Functional imaging. A strong contralateral BOLD activation was found after unilateral acoustic stimulation of either ear before surgery (figure). The right/left contralaterality for right-sided stimulation was 1/3.5 and the left/right contralaterality for left-sided stimulation was 1/4.6. One week after surgery, unilateral stimulation of the intact left ear yielded a response that was strongly contralateralized (left/right ratio: 1/48). In contrast, 5 weeks after surgery, unilateral stimulation of the intact left ear produced a BOLD response on the contralateral and on the ipsilateral hemisphere that was similar to that found before surgery (left/right ratio: 1/3.6). One year later, the response to unilateral stimulation was almost bilaterally balanced (left/right: 1/1.3). The progressive balancing of activity is largely a result of increasing the ipsilateral activity rather than decreasing the contralateral activity.

Discussion. The current data trace the time-course of compensatory reorganization in the cortical representation of auditory stimulation after unilateral destruction of the cochlear nerve. It was a unique clinical opportunity to experimentally follow a patient who presented initially with normal hearing and then after postoperative unilateral deafness due to cochlear nerve resection. Because the experimental procedures involve acoustic stimuli and machine noise that have a considerable sound pressure (90 dB), it would be inappropriate to include patients with acute acoustic trauma or other potentially reversible causes of deafness. During normal bilateral auditory function, the patient showed a BOLD response in the primary auditory cortex that corresponded well with that found in normal hearing

subjects. After hearing loss, stimulation of the intact left ear yielded a progressively increasing contralateral activation. We cannot exclude whether the revision mastoidectomy produced an artifact regarding the BOLD signal. However, this would be expected to produce a suppression of measured activity rather than an accentuation. The data are consistent with and extend our previous findings obtained in a group of unilaterally deaf patients who showed a bilateral BOLD response to unilateral stimulation.[1] Qualitatively, the data also correspond with changes found in studies using evoked magnetoencephalographic potentials after sudden hearing loss in humans.[6]

Auditory pathways project to the contralateral as well as to the ipsilateral auditory cortex.[7] A strong contralateral and a weak ipsilateral cortical activation in response to unilateral stimulation and a facilitated activation in response to binaural stimulation have been shown in humans[1-3] and in animals.[4] The current data suggest that ipsilateral connections, which are normally suppressed, become disinhibited when contralateral inhibitory inputs are removed. However, the exact mechanisms and sites of putative disinhibition are not known. The time-course of reorganization corresponds approximately to that found in animals after experimental lesions.[8-10] The biologic significance of compensatory ipsilateral cortical recruitment remains to be elucidated. Bilateral cortical activation appears to play a role in behaviorally important functional domains including language processing, spatial encoding, and recognition and for the integrity of descending circuits including connections with subcortical systems.

References

1. Scheffler K, Bilecen D, Schmid N, Tschopp K, Seelig J. Auditory cortical responses in hearing subjects and unilateral deaf patients as detected by functional magnetic resonance imaging. Cerebral Cortex 1998;8:156–163.
2. Loveless N, Vasama J, Mäkelä J, Hari R. Human auditory cortical mechanisms of sound lateralisation: III. Monaural and binaural shift responses. Hear Res 1994;81:91–99.
3. Tiihonen J, Hari R, Kaukoranta E, Kajola M. Interaural interaction in the human auditory cortex. Audiology 1989;28:37–48.
4. Brown MC, Kujawa SG, Duca ML. Single olivocochlear neurons in the guinea pig. I. Binaural facilitation of responses to high-level noise. J Neurophysiol 1998;79:3077–3087.
5. Konishi M, Takahashi TT, Wagner H, Sullivan WE, Sullivan WE, Carr CE. Neurophysiological and anatomical substrates of sound localization in the owl. In: Edelman GM, Gall WE, Cowan WM, eds. Auditory Function: Neurobiological Bases of Hearing. New York: Wiley, 1988:721–745.
6. Vasama J, Mäkelä J, Pyykko I, Hari R. Abrupt unilateral deafness modifies function of human auditory pathways. Neuroreport 1995;6:961–964.
7. McMullen NT, De Venecia RK. Thalamocortical patches in auditory neocortex. Brain Res 1993;620:317–322.
8. Robertson D, Irvine DRF. Plasticity of frequency organization in auditory cortex of guinea pigs with partial unilateral deafness. J Comp Neurol 1989;282:456–471.
9. Schwaber MK, Garraghty PE, Kaas JH. Neuroplasticity of the adult primate auditory cortex following cochlear hearing loss. Am J Otol 1993;14:252–258.
10. Rajan R, Irvine DRF, Wise LZ, Heil P. Effect of unilateral partial cochlear lesions in adult cats on the representation of lesioned and unlesioned cochleas in primary auditory cortex. J Comp Neurol 1993;338:17–49.

Neurology®

Cortical reorganization after acute unilateral hearing loss traced by fMRI
D. Bilecen, E. Seifritz, E.W. Radü, et al.
Neurology 2000;54;765
DOI 10.1212/WNL.54.3.765

This information is current as of February 8, 2000

Updated Information & Services	including high resolution figures, can be found at: http://www.neurology.org/content/54/3/765.full.html
References	This article cites 9 articles, 2 of which you can access for free at: http://www.neurology.org/content/54/3/765.full.html##ref-list-1
Citations	This article has been cited by 2 HighWire-hosted articles: http://www.neurology.org/content/54/3/765.full.html##otherarticles
Permissions & Licensing	Information about reproducing this article in parts (figures,tables) or in its entirety can be found online at: http://www.neurology.org/misc/about.xhtml#permissions
Reprints	Information about ordering reprints can be found online: http://www.neurology.org/misc/addir.xhtml#reprintsus

Neurology ® is the official journal of the American Academy of Neurology. Published continuously since 1951, it is now a weekly with 48 issues per year. Copyright . All rights reserved. Print ISSN: 0028-3878. Online ISSN: 1526-632X.

AMERICAN ACADEMY OF NEUROLOGY®